https://doi.org/10.5194/egusphere-2026-5894
Preprint. Discussion started: 18 November 2026
© Author(s) 2026. CC BY 4.0 License.

Large variability in aerosol size distribution, chemical composition, and ice nucleating particles over open water and sea ice in the Arctic during melt season

Babu Suja Arun[1], Heike Wex[1], Thomas Müller[1], Mira L. Pöhlker[1,2], Manuela van Pinxteren[1], Andreas Held[3], Theresa Mathes[1,3], Sabine Lüchtrath[3], Philipp Oehlke[1], Jonas Schaefer[1], Christopher Pöhlker[4,5], Andreas Walbröl[6], Janna E. Rückert[7], Maik Merkel[1], Sebastian Zeppenfeld[1], Susan Hartmann[1], Birgit Wehner[1]

[1]Leibniz Institute for Tropospheric Research, Leipzig, Germany
[2]Leipzig Institute for Meteorology, Leipzig University, Leipzig, Germany
[3]Environmental Chemistry and Air Research, Technische Universität Berlin, Berlin, Germany
[4]Multiphase Chemistry Department, Max Planck Institute for Chemistry, Mainz, Germany
[5]Physikalisch-Technische Bundesanstalt, Braunschweig, Germany
[6]Institute for Geophysics and Meteorology, University of Cologne, Germany
[7]Institute of Environmental Physics, University of Bremen, Bremen, Germany

Correspondence: Babu Suja Arun (arun.babu@tropos.de)

Abstract

Arctic aerosol particles influence climate directly by interacting with radiation and indirectly by modifying cloud properties, including through their role as ice-nucleating particles (INPs). However, their spatio-temporal variability, chemical composition, and climate-relevant properties over open water, marginal ice zone (MIZ), and pack-ice remain poorly constrained. We investigated aerosol particle size distribution, chemical composition (in ambient air and fog), and INPs (in ambient air, fog, sea-ice, melt-pond, and bulk seawater (BSW)) during ATWAICE (ATlantic WAter pathways to the ICE in the Nansen basin and Fram Strait) expedition aboard RV *Polarstern* in summer 2022. Aerosol particles over the ice-free ocean were strongly influenced by primary marine emissions, whereas MIZ and pack-ice environments showed larger contributions from aged/secondary aerosol. Fog water composition indicated direct sea-spray activation and scavenging over ice-free ocean, while MIZ and pack-ice fog contained stronger signatures of sea-ice associated dissolved organic matter. INPs in ambient air were found ~43 m^{-3} at -10°C. INPs in air and fog were predominantly heat-labile, consistent with biological material, whereas BSW, melt-pond, and sea-ice samples contained heat-labile and heat-stable INPs. Case studies combining particle concentration profiles with INP spectra did not indicate a simple and straight forward relationship between INPs and local marine sources. A net emission case (2.2 x 10^6 m^{-2} s^{-1}) showed comparable heat-labile INP fractions in air and BSW, consistent with bubble-bursting or sea-spray production. Conversely, deposition over ice-floes (-0.054 x 10^6 m^{-2} s^{-1}) coincided with ice-active, heat-labile atmospheric INPs absent from BSW, indicating upwind sources, particularly the MIZ and pack-ice environment.

https://doi.org/10.5194/egusphere-2026-5894
Preprint. Discussion started: 18 November 2026
© Author(s) 2026. CC BY 4.0 License.

1. Introduction

Ongoing global climate change is altering the Arctic climate, with wide ranging implications for the atmosphere, ocean, cryosphere, and ecosystems (IPCC, 2019, 2022; Schuur et al., 2022; Grémillet and Descamps, 2023; Wendisch et al., 2023; AMAP 2024). Near surface air temperatures in the Arctic have increased more rapidly than the global mean, a phenomenon commonly termed as Arctic amplification (Serreze and Barry, 2011; Previdi et al., 2021; Rantanen et al., 2022). Since the Arctic is strongly coupled to the broader climate system, changes occurring in these northern high latitudes can even influence processes beyond the Arctic (Cohen et al., 2020). Atmospheric aerosols play a major role in the Arctic, through their ability to interact directly with solar and terrestrial radiation (through light scattering and absorption) and indirectly affect climate by acting as cloud condensation nuclei (CCNs) and ice-nucleating particles (INPs), thereby influencing cloud droplet number concentrations, ice formation, cloud phase, lifetime, and precipitation processes (Abbatt et al., 2019; Wex et al., 2019; Schmale et al., 2021; Li et al., 2022; Burrows et al., 2022).

The surface heterogeneity in the Arctic increases during the summer melt season, when snow and sea ice transition to bare ice, melt-ponds, leads, marginal ice zone (MIZ), and open water (Stroeve et al., 2012). These rapidly evolving conditions influence aerosol emissions, atmospheric processing, and aerosol-cloud-radiation interactions (Galí et al., 2021; Willis et al., 2018; Schmale et al., 2021). Surface type can directly regulate near surface particle exchange in the high Arctic. Flux measurements over contrasting sea-ice environments indicated that wide leads can act as particle sources, whereas closed ice surfaces may function as particle sinks (Mathes et al., 2025). Open leads, snow covered sea ice, and melt-ponds may serve as reservoirs or emission pathways for organic matter, sea-salt, biological material, and other climate-relevant aerosol constituents (Held et al., 2011; Tjernström et al., 2014; Willis et al., 2018; Leon-Marcos et al., 2026). Summer sea-ice retreat can further modify marine aerosol production by influencing air-sea exchange, sea spray generation, and the release of biogenic precursor gases and organic material from oceanic and sea-ice associated ecosystems (Willis et al., 2018; Heutte et al., 2025a). Observational and modeling studies indicate that new particle formation and its subsequent influence on CCNs can occur in association with open water and melting sea ice, suggesting that evolving sea-ice conditions can substantially alter the summertime Arctic aerosol population (Galí et al., 2021; Leck et al., 2025). These changes in aerosol properties are climatically important because persistent Arctic mixed-phase clouds are sensitive to the availability and properties of CCNs and INPs. Variations in aerosol abundance, size distribution, chemical composition, hygroscopicity, and ice-nucleating ability can therefore modify cloud droplet and ice crystal formation, cloud phase and persistence, radiative properties, and the surface energy budget (Shupe., 2011; Creamean et al., 2022; Heutte et al., 2025b).

Fog is a prevalent summer feature in the Arctic, where fog droplets efficiently scavenge particles and dissolve trace gases, facilitating in-droplet aqueous-phase oxidation that generates secondary inorganic and organic components (Heutte et al., 2025a). Fog can modify particle size, composition, and mixing state, thereby altering the availability of CCNs (Noone et al., 1992; Ervens et al., 2011; Zhao et al., 2022; Zeppenfeld et al., 2023). For example, particles may grow during fog events, making it easier for them to act as CCN afterwards (Kecorius et al., 2023). But fog can also function as an aerosol sink, as the deposition flux of fog droplets surpasses that of aerosol dry deposition (Bergin et al., 1995). Guy et al. (2023) found evidence that fog-induced mixing can increase

https://doi.org/10.5194/egusphere-2026-5894
Preprint. Discussion started: 18 November 2026
© Author(s) 2026. CC BY 4.0 License.

near-surface aerosol particle number concentrations. Recent Arctic measurements comparing total and interstitial aerosol during fog periods showed that fog-activated organic aerosol was more oxidized than the non-activated fraction, suggesting that highly oxygenated organic aerosol can be efficiently incorporated into cloud/ fog droplets (Heutte et al., 2025a). This highlights the importance of aerosol and fog water measurements in the Arctic marine boundary layer.

INPs are another climatically important component in the Arctic, since mixed-phase clouds are widespread and persistent in the high Arctic (Morrison et al., 2012; Gierens et al., 2020; Griesche et al., 2026). INPs initiate primary ice formation at temperatures warmer than those required for homogeneous freezing, thereby influencing cloud phase, precipitation formation, cloud lifetime, and radiative effects. However, Arctic INP studies are limited, especially in remote marine and sea-ice covered environments (Hartmann et al., 2021; Barry et al., 2025; Creamean et al., 2022). Recent Arctic observations further indicate that INPs active at relatively high temperature may often be associated with biogenic material (Hartmann et al., 2021; Pereira Freitas et al., 2023; Gratzl et al., 2025; Mavis et al., 2026). These findings show the necessity of measuring INPs in the Arctic not only in ambient air but also in different additional environmental compartments, including sea water, sea ice, fog water, and melt-ponds to learn more about INP type and sources.

Recent decades have experienced numerous studies on aerosol research in the Arctic region based on ground-based observatories, and measurements based on aircraft, shipborne, and balloon-borne platforms (Hartmann et al., 2021; Gogoi et al., 2021; Boyer et al., 2023; Zieger et al., 2023; Jurányi et al., 2023; Pilz et al., 2024; Heutte et al., 2025a, Mavis et al., 2026). However, knowledge of the spatiotemporal variability of climate-relevant properties across the Arctic marine boundary layer's pack ice, MIZ, and open ocean environments, with a focus on distinct environmental compartments such as ambient air, sea water, sea ice, melt-ponds, and fog are limited. This knowledge gap limits our ability to assess aerosol impacts on Arctic clouds, radiation, and climate feedbacks, especially during the biologically active and rapidly evolving summer melt season. Measurements restricted to ambient aerosol alone may not fully resolve the processes linking ice-free ocean, sea ice, melt-ponds, fog, and the MIZ to cloud-relevant aerosol populations. Therefore, simultaneous or coordinated measurements of ambient air, fog water, seawater, sea ice, and melt-ponds are essential for evaluating the relative influence of local marine sources, cryospheric reservoirs, atmospheric processing, and long-range transport. Shipborne campaigns are well suited to address these gaps because they allow measurements across contrasting Arctic surfaces, including open ocean, MIZ, and consolidated pack ice.

This motivated us to conduct the aerosol measurements aboard RV *Polarstern* during the ATWAICE (ATlantic WAter pathways to the ICE in the Nansen basin and Fram Strait) cruise from June to August 2022. Our measurement strategy targeted the Arctic marine boundary layer across different surface types, including the open ocean, MIZ, and consolidated ice pack, and under different synoptic scale airmass conditions. We combined continuous online measurements of aerosol properties with targeted offline sampling of air, fog water, seawater, sea ice, and melt-ponds to investigate climate-relevant aerosol properties and chemical composition. This manuscript presents an integrated overview of observations during ATWAICE. The specific objectives of this study are to: (i) understand the optical properties and size distribution of aerosols in the Arctic across variable surface types and meteorological regimes; (ii) investigate the chemical composition of ambient aerosols and fog

https://doi.org/10.5194/egusphere-2026-5894
Preprint. Discussion started: 18 November 2026
© Author(s) 2026. CC BY 4.0 License.

water; and (iii) investigate INPs in distinct environmental compartments such as ambient air, fog water, seawater, sea ice, and melt-ponds in the Arctic. The results of this study provide a detailed investigation of summertime Arctic marine boundary-layer aerosol variability and deliver insights needed to reduce model uncertainty in the rapidly changing Arctic.

2. Experimental details and methodology

2.1 Campaign overview and experimental setup

The aerosol measurements were made from 29th June to 12th August 2022 during the ATWAICE cruise in the central Arctic aboard the German icebreaker *Polarstern* (PS131). The ship track during the expedition is shown in Figure 1(a) and the experimental set up during the campaign is shown in Figure 1(b). The expedition started from Bremerhaven in Germany, and RV *Polarstern* traversed through the North Sea, Norwegian Sea, Central Arctic Ocean, and Greenland Sea. More details about the ATWAICE expedition are described in Kanzow et al., (2023), and Arun et al. (2026).

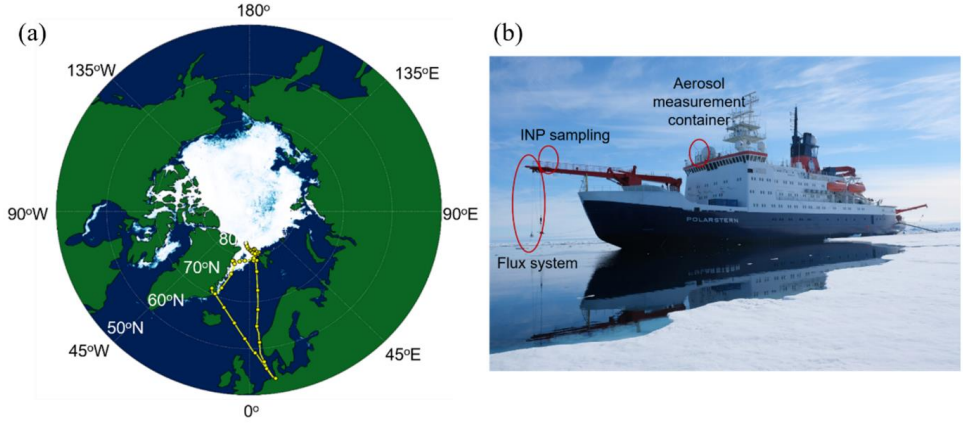


Figure 1. (a) Cruise track of RV *Polarstern*. The white background represents Arctic sea ice concentration data from MODIS-AMSR2, and the yellow dots mark the vessel's position at midday each day. (b) Aerosol measurement setup during ATWAICE.

A laboratory aerosol measurement container equipped with online instrumentation was installed on the observation deck of RV *Polarstern* for near-real time characterization of aerosol particles. A high-volume aerosol sampler (Digitel, PM_{10}) was operated on the rooftop of the aerosol measurement container to collect daily ambient filter samples on quartz fiber filters along with a wind sensor to avoid contamination from the ship for offline chemical characterization during this period. To account for potential contamination during handling and transport, field blanks were prepared by loading the sampler at the sampling site without drawing air through the system.

Another offline custom-built aerosol filter sampler was operated on the bow crane of the ship to collect ambient aerosol samples for characterizing INP properties. Polycarbonate filters (Whatman Nuclepore, pore size 0.8 mm)

https://doi.org/10.5194/egusphere-2026-5894
Preprint. Discussion started: 18 November 2026
© Author(s) 2026. CC BY 4.0 License.

were used for particle collection, at a flow rate of 30 L/min. The filter sampler was mounted on the bow crane at the ship's forward sampling position. The aerosol filter samples collected for INP analysis were also analysed to characterize the major ionic species.

An aluminium box containing a mixing-type condensation particle counter (MCPC Model 1720, Brechtel, Hayward, CA, USA) was lowered by an electric winch from a purpose-built aluminium frame attached to the front end of the bow crane outrigger of RV *Polarstern*. Total particle number concentrations were measured with the MCPC with a lower cut-off diameter of 7 nm and a time resolution of 1 Hz. Measurements were taken at four to eight different height levels from 0.6 m to 11 m above the surface for 5 min each. Particle fluxes were analysed according to the flux-gradient relationship method (Mathes et al. 2025). The custom-made filter sampler was always operated simultaneously to the flux measurements.

Frequent fog events were observed during the expedition period. During these events, fog water was collected using a Caltech Active Strand Cloud Collector, version 2 (CASCC2; Demoz et al., 1996), placed above the rooftop of the aerosol measurement container. The instrument pulls air across Teflon® strands. Droplets strike the strands and drain by gravity into a pre-rinsed Nalgene polyethylene bottle. The fog water collector was switched on whenever visibility dropped markedly and ran continuously through each fog episode. After each fog episode, the collector was rinsed with ultrapure Milli-Q water. These fog water samples were used to characterize the chemical composition, and INP properties in the fog water.

Further, bulk seawater (BSW) samples were collected during each operation of the INP sampler at the beginning and end of each INP sample. BSW samples were drawn from a single outlet of RV *Polarstern* flow through the seawater system at ~11 m depth. In addition, sea ice and melt-pond samples were collected for INP characterization during the campaign. The collected ambient aerosol filter samples, fog water, BSW, sea ice, and melt-pond samples allowed us to assess INPs across these multiple environmental compartments. All samples were stored at -20 °C immediately after sampling and transported frozen to TROPOS for offline laboratory analysis.

2.2 Measurements of physical and optical properties of aerosol particles

Aerosol particle number size distributions in the range of 10 - 800 nm were measured every 5 min using a TROPOS-type Mobility Particle Size Spectrometer (MPSS) (Wiedensohler et al., 2012). The MPSS setup consisted of a Hauke-type Differential Mobility Analyzer with an effective length of 28 cm, a Condensation Particle Counter (CPC, model 3010, TSI Inc., USA) operating at a sample flow rate of 1 L min^{-1}. The raw electrical mobility distributions obtained from the MPSS were converted into particle number size distributions using the inversion algorithm developed by Pfeifer et al. (2014). The sizing accuracy of the MPSS was validated using monodisperse polystyrene latex spheres with a diameter of 203 nm (Thermo Scientific™ Duke Standards™).

Light scattering coefficients (σ_{sca}) measurements were conducted using a three-wavelength integrating Nephelometer (Aurora Ecotech 4000). Details regarding its measurement principle and correction factors are provided in Müller et al. (2011). Further, refractory black carbon (rBC) measurements were made using a single particle soot photometer (SP2-D). More details on these measurements are provided in Arun et al. (2026).

https://doi.org/10.5194/egusphere-2026-5894
Preprint. Discussion started: 18 November 2026
© Author(s) 2026. CC BY 4.0 License.

2.3 Chemical characterization of aerosol particles and fog water

The concentrations of selected inorganic (SO_4^{2-}, NO_3^-, Cl^-, Na^+, NH_4^+, K^+, Mg^{2+}, Ca^{2+}) and organic ions ($C_2O_4^{2-}$, formate, MSA^-) were determined in filtered aqueous PM_{10} extracts and cloud water samples (0.45 µm syringe filters) using ion chromatography and conductivity detection (Dionex ICS-6000, Thermo Scientific). The cations were separated in an isocratic mode (eluent: 36 mM methanesulfonic acid) on a Dionex IonPac CS16-4µm column (2×250 mm) that was combined with a Dionex IonPac CG16-4µm guard column (2×50 mm). Anions were separated on a Dionex IonPac AS18 column (2mm250 mm) with an AG18 guard column (2mm50 mm), using a potassium hydroxide (KOH) gradient as described in Zeppenfeld et al. (2026). The detection limits for the determined ions ranged from 5 to 20 µg L^{-1} (Zeppenfeld et al., 2021).

Since oceanic emissions are the dominant source of atmospheric sodium in marine environments, the contribution of sea-salt sulfate (ss- SO_4^{2-}) was estimated based on the characteristic mass ratio of $SO_4^{2-}/Na^+ = 0.251$ in bulk seawater (Millero and Sohn, 1992). The fraction of non-sea-salt sulfate (nss-SO_4^{2-}) was determined by subtracting the ss-SO_4^{2-} from the total SO_4^{2-} concentration.

Organic carbon (OC) and elemental carbon (EC) were measured with a Sunset Laboratory Dual-Optical Carbon Analyzer using the EUSAAR 2 protocol with laser-based charring correction (Cavalli et al., 2010). Water soluble organic carbon (WSOC) was determined in filtered aqueous PM_{10} extracts and cloud water samples (0.45 µm syringe filters) using a Shimadzu TOC-VCPH after carbonate removal by acidification and purging. CO_2 was quantified by NDIR detection with external calibration. More details on the methods can be found in Müller et al. (2010) and van Pinxteren et al. (2017). The organic matter concentration in this study is estimated as, OM=1.8 × OC and dissolved organic matter (DOM) as DOM=DOC x 1.8.

2.4 Measurements of Ice Nucleating Particles

INP spectra were derived using the Leipzig Ice Nucleation Array (LINA) and the Ice Nucleation Droplet Array (INDA), both of which have been used and described previously (Hartmann et al., 2021; Sze et al., 2023). To test for heat-labile INPs, each sample was heated to 90 °C for 30 min, and the INP spectra were measured with INDA. Heating can lower ice activity because many biological INPs rely on proteins that lose function at high temperatures (Pummer et al., 2012; Hill et al., 2016).

We computed the cumulative INP number concentration $N_{INP}\ (T)$ as a function of temperature following Vali (1971) as,

$$N_{\mathrm{INP}}(T) = -\frac{\ln(1 - f_{frozen}(T))}{V}$$

where the frozen fraction f_{frozen} is,

$$f_{frozen}(T) = \frac{N(T)}{N_{\mathrm{Total}}}$$

https://doi.org/10.5194/egusphere-2026-5894
Preprint. Discussion started: 18 November 2026
© Author(s) 2026. CC BY 4.0 License.

Here, N(T) is the number of droplets frozen at temperature T, and N_{Total} is the number of droplets examined.

For filter samples reported per volume of air, the reference volume V is the air-equivalent volume contained in one droplet and is calculated as:

$$V = \frac{V_{\text{air}}}{V_{\text{water}}} . V_{\text{droplet}}$$

V_{air} is the total air drawn through a filter, V_{water} is the extraction volume for washing the filter and V_{droplet} is the volume of a single droplet (1 µL for LINA; 50 µL for INDA).

For the liquid samples such as BSW, sea ice samples, melt-pond samples, and fog water samples, we derived INP concentrations per volume of examined liquid, using the same formula but set,

$$V = V_{droplet}$$

We calculated heat-labile fraction $f_{\text{heat labile}}$ as function of temperature using the unheated and heated INP number concentrations:

$$f_{\text{heat liable}}(T) = 1 - \frac{N_{\text{heated INP}}(T)}{N_{\text{INP}}(T)}$$

Values close to 1 indicate that most INPs became inactive after heating (highly heat-labile, likely biological), whereas values near 0 indicate little effect of heating (lowly heat-labile).

2.5 Airmass back trajectories and source attribution

Five-day airmass back trajectories were calculated for this study using NOAA Hybrid Single-Particle Lagrangian Integrated Trajectory model (HYSPLIT) (Stein et al., 2015) (~ 100 m a.s.l.) as shown in Fig. S1. Further, Arctic Sea ice concentration data from MODIS-AMSR2 (1 km resolution; Spreen et al., 2008; Ludwig et al., 2020) were also used to understand the surface types of these airmass pathways. We define the MIZ as the zone between open water and consolidated pack ice where sea-ice cover is ~15-80%. Furthermore, in order to explain the aerosol properties in relation to surface types, we categorized open water areas as ice-free ocean, MIZ, and pack ice based on sea ice concentration data, and our visual observations during the campaign. For PM_{10} samples collected from different surfaces, we assigned the surface type that dominated the sampling interval, since each filter integrates over several hours while the ship is underway.

3. Results and Discussion

3.1 Aerosol particle number size distribution and optical properties

Figure 2 shows the particle number size distribution, integrated particle number concentrations in different size ranges (nucleation: $N_{<25\ nm}$, Aitken: $N_{25\text{-}100\ nm}$, and total, $N_{100\text{-}800\ nm}$), and fractional contributions (nucleation, Aitken, and accumulation, $N_{100\text{-}800\ nm}$), light scattering coefficient, and rBC mass concentration during the study

https://doi.org/10.5194/egusphere-2026-5894
Preprint. Discussion started: 18 November 2026
© Author(s) 2026. CC BY 4.0 License.

period. Total number concentrations varied from < 10 cm^{-3} to ~8000 cm^{-3} with pronounced concentrations associated with either new particle formation or episodic aerosol transport such as warm airmass intrusions. The higher abundance of particles (often >4000 cm^{-3}) at the beginning of the campaign, before entering the Arctic circle, reflects strong influence from the European anthropogenic influences, including emissions from ship traffic corridors. This is also in line with the higher values of $\sigma_{sca,525nm}$ (37 ± 16 Mm^{-1}) and rBC mass concentrations (71 ± 47 ng m^{-3}) observed during this period. The higher values of $\sigma_{sca,525nm}$ during this period may also have been due to sea spray aerosols, since RV *Polarstern* was traversing completely through open ocean waters.

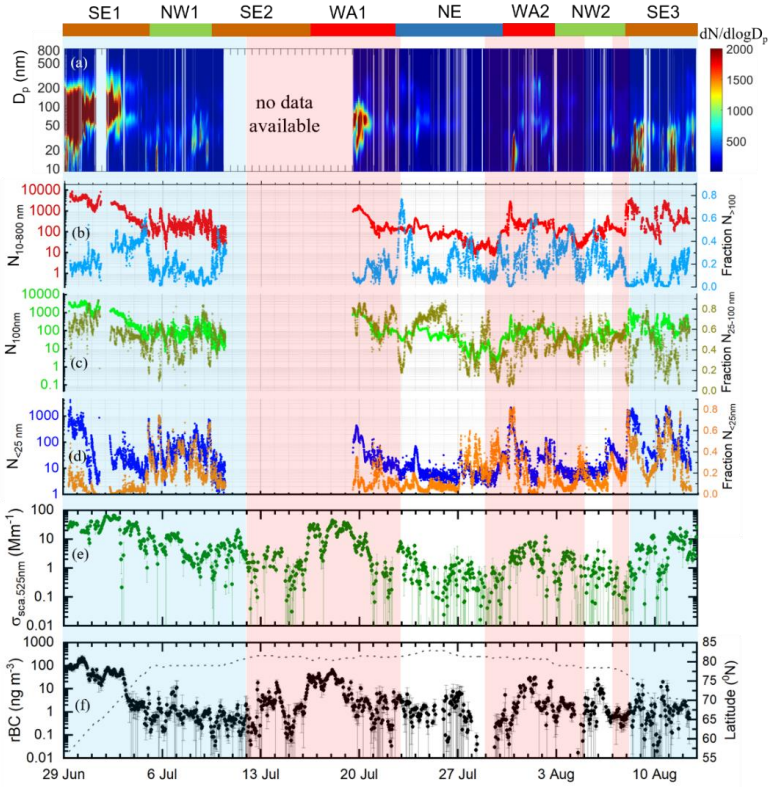


Figure-2: (a) Particle number size distribution derived from MPSS (10-800 nm), (b) Total number concentration $N_{10\text{-}800\ nm}$ (left y-axis) and fraction of particles >100 nm (right y-axis), (c) Number concentration $N_{25\text{-}100\ nm}$ (left y-axis) and fraction in the 25-100 nm range (right y-axis), (d) Number concentration $N_{10\text{-}25\ nm}$ (left y-axis) and fraction 10nm - 25 nm (right y-axis), (e) Aerosol light scattering coefficient at 525 nm, ($\sigma_{sca,525\ nm,}$ Mm^{-1}), (f) Refractory black carbon mass concentration in ng m^{-3} (left y-axis), and corresponding latitudes of RV *Polarstern* (dotted lines, right y-axis). The background colors indicate the major surface type encountered by RV *Polarstern* during the expedition. (blue= ice-free ocean, red= marginal ice zone, white= pack ice). The top labels indicate the influence of eight distinct airmasses during the cruise (SE1= South easterly 1; NW1= North westerly 1; SE2=South easterly 2; WA1= Warm airmass intrusion 1; NE=North easterly; WA2= Warm airmass intrusion 2; NW2= North westerly 2; SE3= South easterly 3 as shown in Fig. S1).

https://doi.org/10.5194/egusphere-2026-5894
Preprint. Discussion started: 18 November 2026
© Author(s) 2026. CC BY 4.0 License.

We found distinct airmass influence on aerosol properties during the campaign, as evidenced by eight continuous airmass regimes shown in Fig. S1. The surface types over which the observed distinct airmasses were traversing, along with their percentages, are shown in Fig. S2. Further, we observed two warm airmass intrusion periods (WA) during the study period, as shown in Fig. S3. Most airmasses had a strong marine influence, particularly from the ice-free ocean, but the relative contributions of ice-free ocean, MIZ, pack ice, and continental influence varied by airmass sector.

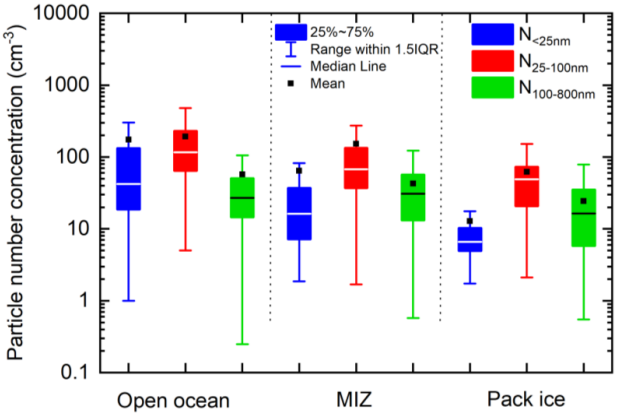


Figure-3: Aerosol particle number concentration (cm^{-3}) determined at different size ranges in each surface conditions during cruise.

Over the ice-free ocean within the Arctic (from 3rd of July onwards), before the RV *Polarstern* entered the MIZ region, the particle concentrations were mostly contributed by the Aitken mode particles (151 ± 168 cm^{-3}) in addition to the dominant contributions of accumulation mode aerosols ($N_{100\text{-}800nm}$) (69 ± 118 cm^{-3}) ((Fig. 2). These periods were influenced by airmasses traversing mainly from the north westerly and south easterly direction with most of them traversing over the open ocean environments (NW1, SE1 and SE2 in Fig. S1 and Fig. S2). The elevated particle concentrations observed in this open ocean environments may reflect contributions from both primary and secondary marine aerosols. Wave breaking and bubble bursting provide a direct source of primary sea spray particles (Held 2011), and recent Arctic observations have linked enhanced aerosol concentrations over open water to sea state conditions (Moallemi et al., 2024; Simon et al., 2025). At the same time, oxidation of ocean derived gaseous precursors can produce secondary marine particles that coexist with sea spray aerosol and may contribute efficiently to the cloud relevant submicron population (De Leeuw et al., 2011; Moallemi et al., 2024).

While RV *Polarstern* entered the MIZ, total particle number concentrations were decreased together with a reduction in Aitken and accumulation mode particle concentrations, rarely accompanied by nucleation mode particles. Previous studies (Heintzenberg et al., 2015; Kecorius et al., 2019) indicated that, the surface characteristic transition, from open water to ice-influenced surfaces, plays an important role in the aerosol budget over the Arctic region, since secondary particle formation and growth become prominent as MIZ/open-lead biogeochemistry and sea-ice melt drive particle formation and growth. It was noted that, during warm airmass intrusion periods (WA1 and WA2), the airmasses were traversing mostly from south easterly directions (Fig. S1)

https://doi.org/10.5194/egusphere-2026-5894
Preprint. Discussion started: 18 November 2026
© Author(s) 2026. CC BY 4.0 License.

with significant contributions from Eastern Siberia (WA1). During these events, total particle number concentrations increased substantially, accompanied by enhanced σ_{sca} (12 ± 12 Mm^{-1}), and rBC (12 ± 15 ng m^{-3}). Unfortunately, due to technical issues the MPSS data were mostly missing during WA1.

The lowest particle number concentrations were observed while the RV *Polarstern* was traversing through pack ice environments. Nucleation-mode number concentrations were found to be lower in comparison to MIZ, yet Aitken mode fractions were modestly enhanced relative to the open ocean/MIZ environments (Fig.2c). We also found the lowest σ_{sca} (0.7± 1.2 Mm^{-1}) and rBC (1.3 ± 1.6 ng m^{-3}) during these periods. More details on σ_{sca}, rBC properties, and mixing state during the campaign are discussed in Arun et al. (2026). At the end of the observational period, we observed larger contribution in nucleation mode particles over the ice-free oceanic environments. This contributes to the larger fraction of $N_{<25nm}$ in Fig. 3 while considering combined ice-free oceanic regions. Overall, the particle size distribution during the cruise indicated dominance of Aitken mode particles (Fig. 3) in all the surface regimes.

3.2 Variability in chemical characteristics of ambient aerosol particles and fog water

3.2.1 Chemical composition of ambient aerosol particles (PM_{10})

Figure 4 and Table S1 summarize the spatial and temporal variability in aerosol chemical composition during the cruise. Before the vessel crossed the Arctic circle (before 3rd of July), aerosol species concentrations were high, consistent with the particle number, σ_{sca}, and rBC concentrations reported above. The proximity of RV *Polarstern* to European source regions indicates a predominantly continental anthropogenic influence during this period. Within the Arctic Ocean (from 3rd July onwards), the mass concentrations decreased, consistent with weaker primary anthropogenic sources and scavenging during long-range atmospheric transport. Over the ice-free ocean, the mass fraction of the chemical composition is dominated by Na^+ (21.4 %), Cl^- (33.6 %), OM (24.8 %) and SO_4^{2-} (14.7 %) (Fig.5a) respectively indicating a strong marine contribution.

In the MIZ, OM (47.5 %) and SO_4^{2-} (21.8 %) made the largest contributions (Fig. 5b). Airmasses arrived from the southeast, including warm airmass advection, as well as from the northeast and northwest (Fig. 4 and Fig. S1), therefore the chemical composition reflects both local MIZ sources and transport. The warm airmass intrusion (WA1) increased absolute species concentrations, but the relative composition remained similar to that observed on preceding days.

Above pack ice, aerosol species concentrations were lowest, consistent with a remote, source limited summer boundary layer and efficient scavenging. Most airmasses arrived from the northeast after traversing over pack ice (Fig. 4 and Fig. S1), further limiting primary sources. We also found lower accumulation mode aerosol number concentrations (Fig. 3) in these environments. Previous studies indicated lower accumulation mode number concentrations and frequent ultrafine particle episodes tied to local precursors (eg., iodine, dimethyl sulfide (DMS)) rather than transported anthropogenic aerosol over pack ice conditions (Heintzenberg and Leck., 2012). The lower fractions of Na^+ (3.2 %) and Cl^- (3 %) above the pack ice likely reflect reduced sea-salt production under continuous ice cover, whereas OM (67.8 %) and SO_4^{2-} (19.6 %) dominated the measured mass (Fig. 5c).

https://doi.org/10.5194/egusphere-2026-5894
Preprint. Discussion started: 18 November 2026
© Author(s) 2026. CC BY 4.0 License.

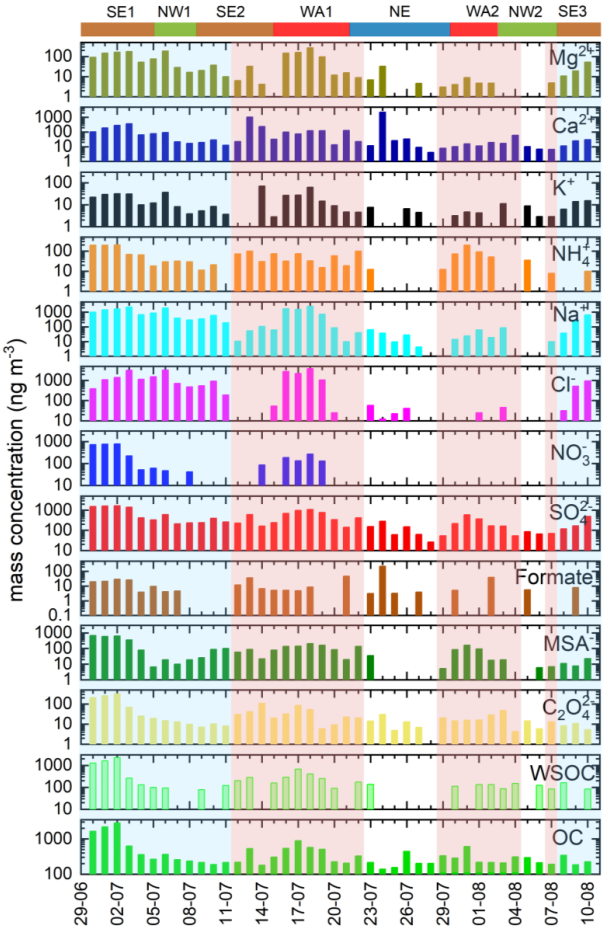


Figure-4: Mass concentrations (ng m^{-3}) of chemical species measured in PM_{10} filter samples. Background colours indicate the surface regimes: blue= ice-free ocean, red= marginal ice zone, white= pack ice. Labels at the top show backward airmass directions.

Figure S4 shows correlations among different chemical species in the aerosol filter samples. Over the ice-free ocean, significant correlations were observed among Cl^-, Na^+, K^+, Mg^{2+} and Ca^{2+}. This suggests the formation of primary sea spray aerosol from open water when bubble bursting transfers inorganic salts originating from seawater into the marine boundary layer (Legrand et al., 2017). Significant correlations of OC with Na^+ (R^2=0.6, $p<0.01$) and the other sea-salt ions may reflect transfer of organic matter from the sea-surface microlayer. By contrast, WSOC strongly correlated with $C_2O_4^{2-}$ (R^2=0.75, $p<0.01$), MSA (R^2=0.78, $p<0.01$), moderately correlated with nss-SO_4^{2-} (R^2=0.65, $p<0.05$), and weakly with Na^+ (R^2=0.2) and Cl^- (R^2=0.13). This indicates that WSOC variability was not primarily controlled by fresh sea spray emissions but was more consistent with a photochemically processed or secondary aerosol component (Ziemba et al., 2011; Singh et al., 2021). Correlations among MSA, nss-SO_4^{2-}, $C_2O_4^{2-}$, and formate further support oxidation of marine DMS and organic precursors,

https://doi.org/10.5194/egusphere-2026-5894
Preprint. Discussion started: 18 November 2026
© Author(s) 2026. CC BY 4.0 License.



followed by aqueous or multiphase processing. The ice-free-ocean aerosol therefore contained both primary sea spray and secondary biogenic material.

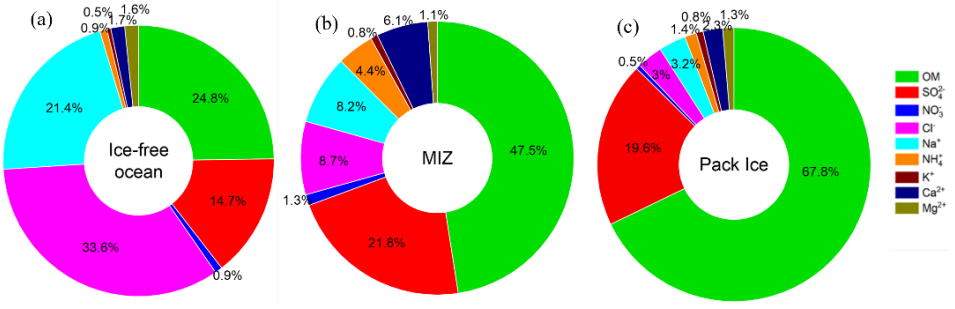


Figure-5 Mass fractions of chemical components in PM_{10} samples collected over (a) the ice-free ocean (n=12), (b) the marginal ice zone (n=19), and (c) pack ice (n=8) during the study.

In the MIZ, correlations of Na^+ with Cl^- ($R^2 = 1$, $p < 0.001$), Mg^{2+} ($R^2 = 0.97$, $p < 0.001$), and K^+ ($R^2 = 0.4$, $p < 0.05$) likewise indicate a substantial sea spray contribution from open water, leads, broken ice, and wind-driven surface processes. WSOC correlated with nss-SO_4^{2-} ($R^2 = 0.5$, $p < 0.01$), $C_2O_4^{2-}$ ($R^2 = 0.7$, $p < 0.001$), and MSA ($R^2 = 0.41$, $p < 0.05$), while OC and WSOC were strongly correlated ($R^2 = 0.91$, $p < 0.001$). Together, these relationships indicate a water-soluble, chemically processed biogenic fraction superimposed on primary sea-salt. This is consistent with increased biological activity near the retreating ice edge, enhanced emission of DMS and organic precursors, and their subsequent condensation or chemical processing on sea-salt particles. The MIZ is a dynamic transition zone containing open water, broken ice, and melt features that can influence marine biological emissions and the sea to air transfer of organic species. Chang et al., (2011) reported that marine biogenic sulfur emissions and subsequent sulfate formation can contribute substantially to the submicron aerosol burden under remote Arctic marine conditions. SO_4^{2-} over the MIZ/pack ice may therefore originate from both atmospheric transport and oxidation of marine sulfur gases, while fog and cloud processing may further modify its production and removal (He et al., 2022; Nilsson & Leck, 2002). The strong correlation between OC and WSOC (R^2=0.91, p<0.001) further indicate that the organic aerosol in the MIZ region contained a substantial water soluble fraction, which would be readily incorporated into fog droplets during activation or scavenging.

Over pack ice, the absence of significant correlations among sea-salt ions indicates a weaker or more variable influence of sea spray and transported airmasses. The weaker Na^+ and Cl^- relationship (R^2=0.43) may reflect both reduced sea spray and chemical aging. In aged marine aerosols, reactions with the anions of acidic species can release HCl and alter the original seawater ionic signature (Hsu et al., 2007). In addition, significant correlations among nss-SO_4^{2-}, $C_2O_4^{2-}$ (R^2=0.93, p<0.001), and formate (R^2=0.88, p<0.01) point to common secondary oxidation. The weaker MSA and nss-SO_4^{2-} relationship suggests that sulfate was not controlled solely by local DMS oxidation and may also include transported sulfate, oxidized SO_2, or sulfur formed under different oxidation conditions. Across the three regimes, the aerosol composition shifted from a strong sea-salt signature over ice-free ocean to an OM rich, secondary influenced composition over pack ice, likely modulates chemical composition of fog during summer melt season.

https://doi.org/10.5194/egusphere-2026-5894
Preprint. Discussion started: 18 November 2026
© Author(s) 2026. CC BY 4.0 License.

3.2.2 Chemical composition of fog water

Figure 6 shows spatio-temporal variabilities in the mass concentration of different chemical species in fog water samples collected during the cruise. The measured chemical species include DOC, organic, and inorganic ions. The mass concentration of these chemical species shows significant variabilities during the cruise (Table S2).

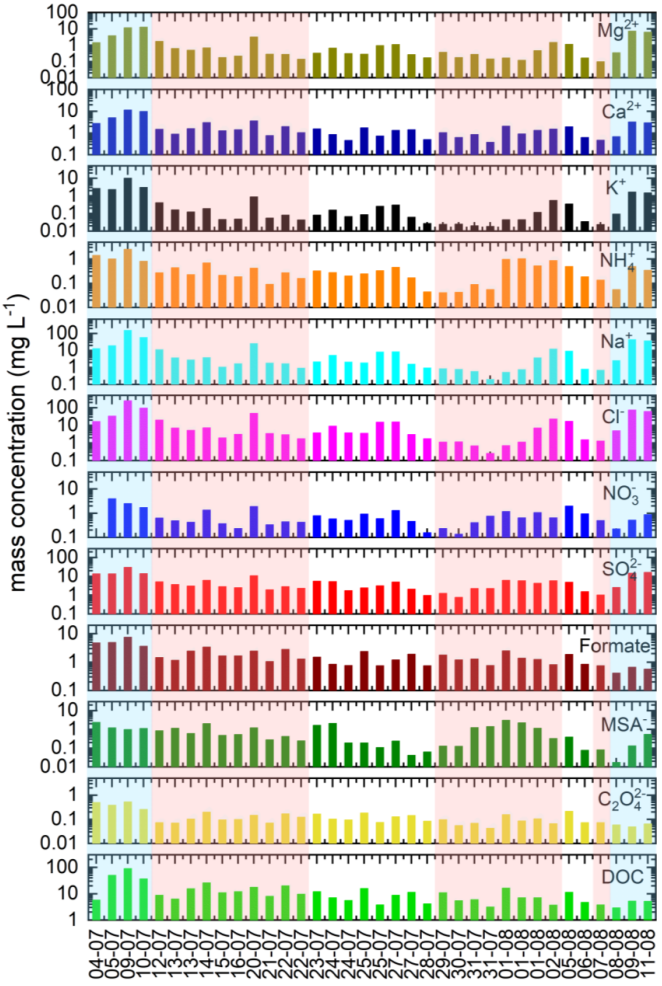


Figure-6: Concentrations of DOC, organic ions, and inorganic ions in fog water samples collected during ATWAICE. Background colours indicate surface regimes: blue= ice-free ocean, red= marginal ice zone, and white= pack ice.

Figure 7 shows the relative mass fractions of DOM and major inorganic ions in the fog water collected over the ice-free ocean, MIZ, and pack ice. DOM, Cl^-, and Na^+ dominated in all three regimes, but their relative contributions changed with surface conditions. DOM increased from 23.4 % over the ice-free ocean to 57.5 % in the MIZ and 50 % over pack ice. Over the same transition, Cl^- reduced from 34.8 % to 14.3 % and 21 %, and Na^+

https://doi.org/10.5194/egusphere-2026-5894
Preprint. Discussion started: 18 November 2026
© Author(s) 2026. CC BY 4.0 License.

from 21.6 % to 8 % and 11 %, respectively. The ice-free ocean fog therefore retained a stronger sea-salt signature, whereas the MIZ and pack ice samples were enriched in DOM, consistent with weaker direct sea spray influence and/or greater contributions from ice associated biological sources and organic rich surface reservoirs (Zeppenfeld et al., 2023). The SO_4^{2-} fraction varied little among regimes (11 %, 11.2 %, and 10 %, respectively; Fig. 7).

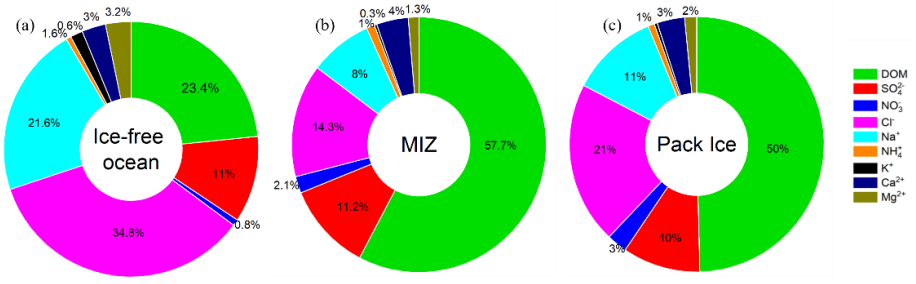


Figure-7: Mass fractions of DOM and inorganic ions relative to their summed concentration in fog water collected over (a) open ocean (n=7), (b) the marginal ice zone (n=19), and (c) pack ice (n=10) environments.

Figure 8 shows correlations among chemical species measured in fog water. Over the ice-free ocean, strong correlations among Na^+, Cl^-, Mg^{2+}, and Ca^{2+} indicate that primary sea-salt particles were activated or scavenged into fog droplets. Their large size and hygroscopicity make these particles efficient fog condensation nuclei, consistent with the sea-salt dominated ambient aerosol. DOC also correlated with Na^+ ($R^2 = 0.7$, $p < 0.05$), Cl^- ($R^2 = 0.7$, $p < 0.05$), Ca^{2+} ($R^2 = 0.75$, $p < 0.05$), and K^+ ($R^2 = 0.8$, $p < 0.01$), linking much of the fog DOM to marine emissions. Correlations of DOC with formate ($R^2 = 0.72$, $p < 0.05$), oxalate with formate ($R^2 = 0.93$, $p < 0.001$), and MSA with nss-SO_4^{2-} ($R^2 = 0.84$, $p < 0.05$) show that soluble secondary products identified in the aerosol were retained in the fog.

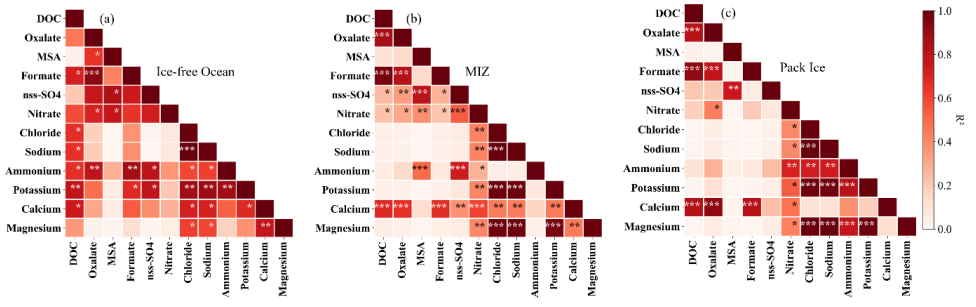


Figure-8: Correlation among chemical components in fog water samples collected over (a) ice-free ocean, (b) the marginal ice zone, and (c) pack ice. Colour shading represents R^2, from 0 (white) to 1 (dark red). Asterisks indicate significance: * $p < 0.05$, ** $p < 0.01$, and *** $p < 0.001$.

In MIZ fog, correlations among Na^+, Cl^-, Mg^{2+}, Ca^{2+}, and K^+ again indicate sea-salt activation. Correlations of DOC with $C_2O_4^{2-}$ ($R^2 = 0.9$, $p < 0.001$) and formate ($R^2 = 0.97$, $p < 0.001$), together with associations of nss-SO_4^{2-} with MSA ($R^2 = 0.8$, $p < 0.001$), NH_4^+ ($R^2 = 0.73$, $p < 0.001$), formate ($R^2 = 0.3$, $p < 0.05$), $C_2O_4^{2-}$ ($R^2 = 0.4$, $p < 0.01$), and NO_3^- ($R^2 = 0.53$, $p < 0.01$), are consistent with an additional chemically processed component.

https://doi.org/10.5194/egusphere-2026-5894
Preprint. Discussion started: 18 November 2026
© Author(s) 2026. CC BY 4.0 License.

Associations of NO_3^- with Na^+ ($R^2 = 0.4$, $p < 0.05$), Cl^- ($R^2 = 0.4$, $p < 0.05$), and Mg^{2+} ($R^2 = 0.43$, $p < 0.05$) in both aerosol and fog further indicate that nitrate was carried on marine particles. The MIZ fog thus reflects primary sea spray, marine biogenic sulfur oxidation, and secondary aerosol processing.

Over pack ice, correlations among Na^+, Cl^-, K^+, and Mg^{2+} show that sea-salt material remained in fog despite its smaller aerosol mass fraction. Selective activation allows even intermittent sea-salt from leads, saline snow, or transported marine aerosol to contribute strongly to fog water ions. The weaker association of DOC with sea-salt tracers than over the ice-free ocean and MIZ suggests additional sources or processing within the sea-ice environment. Strong correlations of DOC with $C_2O_4^{2-}$ ($R^2 = 0.82$, $p < 0.001$) and formate ($R^2 = 0.92$, $p < 0.001$), and of $C_2O_4^{2-}$ with formate ($R^2 = 0.8$, $p < 0.001$), link the dissolved organics to shared sources or atmospheric processing. Possible contributors include marine organic emissions, oxidation before aerosolization, uptake of soluble gases, and aqueous reactions in fog; sea-ice microorganisms and organic-rich surface reservoirs may also act as sources (Zeppenfeld et al., 2023). The MSA and nss-SO_4^{2-} correlation ($R^2 = 0.75$, $p < 0.01$), together with the weak association of MSA with sea-salt tracers, supports a mainly secondary marine sulfur contribution, although nss-SO_4^{2-} may have other sources. Across all regimes, fog retained a sea-salt signature while the organic and sulfur fractions also reflected secondary processing and sea ice associated sources.

3.3 Ice nucleating particles across distinct environmental compartments

3.3.1 INP concentrations in air, seawater, melt-pond, sea ice and fog water

To understand different sources of atmospheric INP population, different environmental compartments were sampled and analysed regarding their ice nucleation activity. Figure 9 shows all temperature resolved N_{INP} spectra of the atmospheric filter samples, BSW, melt-pond, sea ice and fog water collected during the study. Heat labile INPs will be discussed separately in the subsequent section.

As can be seen in Fig. 9(a), N_{INP} of the filter samples spans roughly two to three orders of magnitude at all temperatures, with the largest variability observed at higher temperatures. As expected, N_{INP} increased with decreasing temperature. Highly ice-active INPs were found in several atmospheric filter samples, with N_{INP} reaching up to ~ 4.3×10^1 m^{-3} even at -10 °C. The time series of N_{INP} at selected temperatures, derived from the filter samples, is shown in Fig. S5. While a large variability was found for N_{INP}, some sensitivity to the sea ice environment can be seen. Periods when RV *Polarstern* was located within the MIZ or inside the pack ice environments were characterized by elevated N_{INP} compared to open ocean water environments in most of the samples. At -20 °C, N_{INP} frequently exceeded 100 m^{-3} in the MIZ and pack ice environments, whereas N_{INP} over the open ocean water were generally lower. A similar, although less pronounced pattern is evident at higher temperatures: at -10 and -14 °C, N_{INP} in the MIZ and pack ice were higher, while samples over the open ocean water were mostly lower, particularly at -10 °C.

Further, BSW samples were collected at the beginning and end of each atmospheric filter sampling. Figure 9(b) shows N_{INP} per volume of water in BSW samples collected during the cruise. We did not find significant differences in N_{INP} between the BSW samples collected before and after each atmospheric filter sampling, beyond the general sample-to-sample variability. At any given temperature the spread of N_{INP} in BSW spans roughly one to two orders of magnitude, i.e., showing a smaller spread than seen in the filter samples. Only a few samples

https://doi.org/10.5194/egusphere-2026-5894
Preprint. Discussion started: 18 November 2026
© Author(s) 2026. CC BY 4.0 License.

started to freeze at temperatures above -10 °C. In general, samples collected above the ice pack showed warmer onsets more often (typically ≥ -13 °C), while samples from MIZ and open ocean water sectors more frequently initiated freezing at below -13 °C.

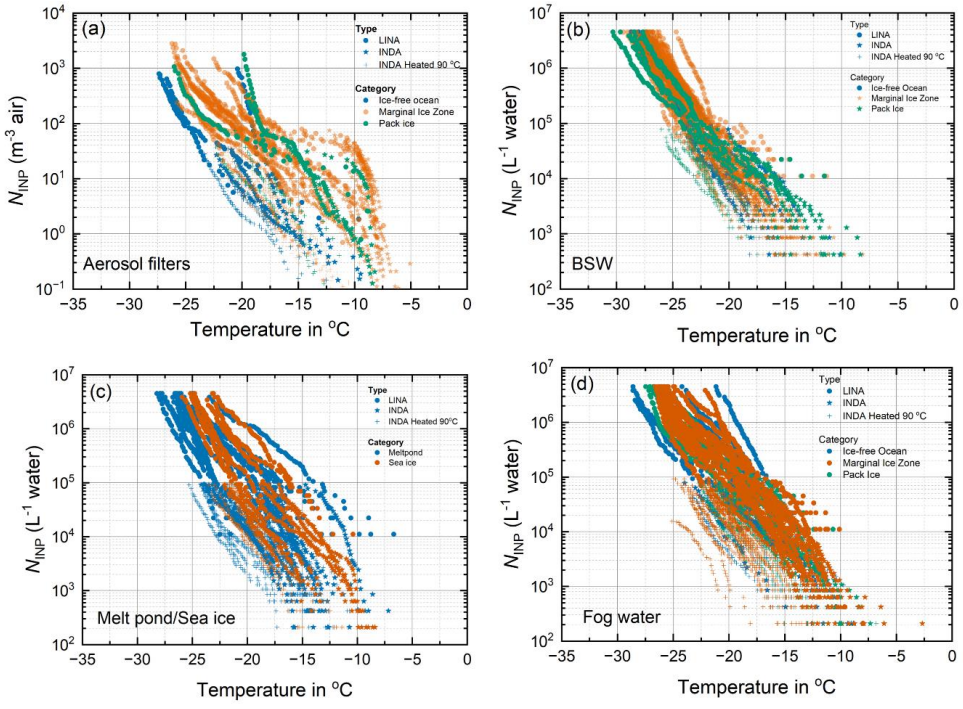


Figure-9: (a) INP spectra from ambient aerosol filter samples collected during ATWAICE; Colours denote the sampling environment: open ocean (blue), marginal ice zone (red), and pack ice (green). Symbols indicate methods/treatments: filled circles represents LINA-derived INPs, asterisks represent INDA derived INPs, and plus symbols represent INDA derived INPs after heating at 90 °C. Panels (b), (c) and (d) show INP spectra for BSW, for melt-ponds and sea ice, and for fog water, respectively.

Figure 9(c) shows the N_{INP} derived from the melt-pond and sea ice samples. N_{INP} exhibited substantial variability, with INP concentrations spanning two to three orders of magnitude at any given temperature. The overlap between the two sample categories of melt-ponds and sea ice indicates that they may contain similar INP populations. Melt-ponds may be an important reservoir of INPs for the Arctic atmosphere. Observed N_{INP} in both melt water and sea ice samples often exceed those of BSW. This is generally pointing to an enrichment of warm-temperature INPs in waters connected to cryosphere surfaces relative to the underlying ocean, which was already observed by Irish et al. (2017).

Figure 9(d) shows N_{INP} as function of temperature derived from fog water. Again, considerable variability was observed among samples, with concentrations differing by several orders of magnitude at any given temperature. This variability likely reflects differences in airmass origin, fog microphysical processing, local surface influence, and the availability of marine, sea ice related, or transported aerosol particles that were activated into fog droplets.

https://doi.org/10.5194/egusphere-2026-5894
Preprint. Discussion started: 18 November 2026
© Author(s) 2026. CC BY 4.0 License.

The different sampling environments broadly showed overlapping ranges of N_{INP}, with a lower relative abundance of highly ice-active INPs compared to atmospheric samples in MIZ and pack ice. This may hint towards a depletion of the most ice-active INPs from the atmosphere through fog formation and subsequent settling. It is interesting to note that the values for N_{INP} of fog are generally in a similar temperature/concentration range as observed for melt-pond, and sea ice samples. Overall, substantial concentrations of INPs active at temperatures as warm as -10 °C were observed only in atmospheric filter samples collected in the MIZ and pack ice environments.

3.3.2 Heat-labile INPs

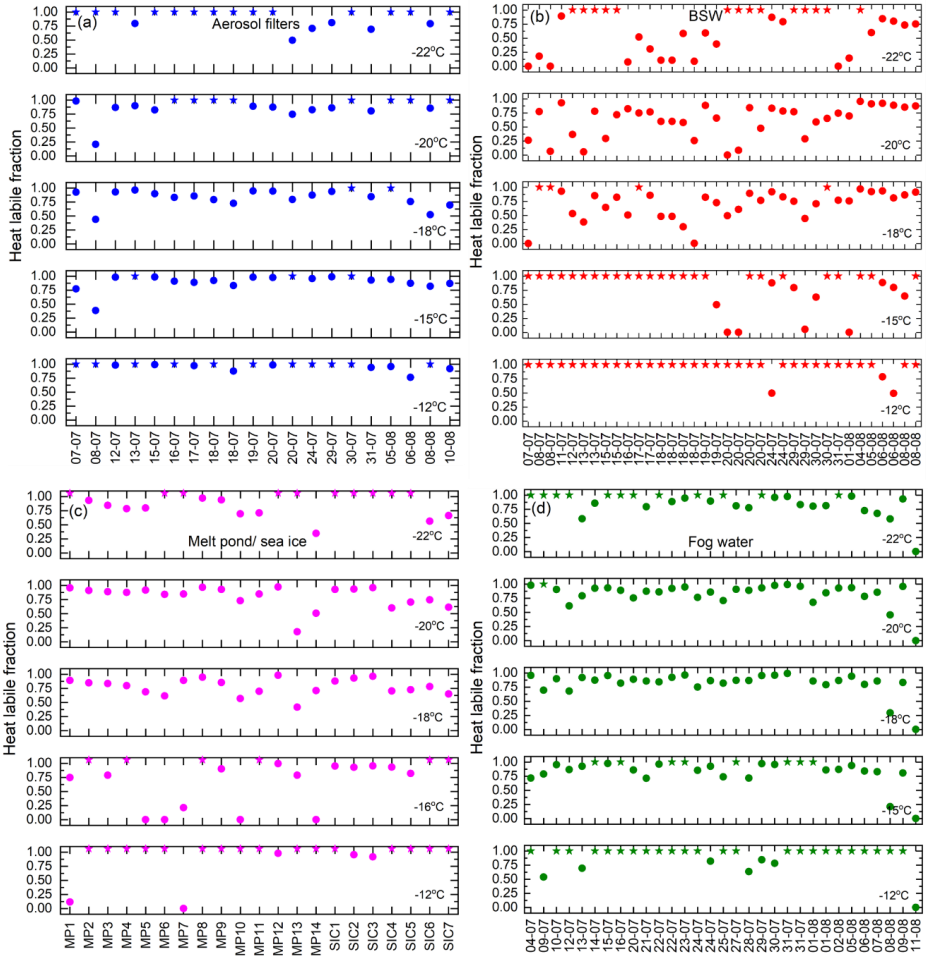


Figure-10: Heat labile fraction of the samples analysed in this study for (a) atmospheric filter samples, (b) bulk seawater samples, (c) melt-pond and sea ice samples, and (d) fog samples. Symbols marked with asterisks denote cases where the heat-labile fraction could not be calculated, or where one of the corresponding values was zero, and these points were therefore not considered in the interpretation of heat sensitivity.

https://doi.org/10.5194/egusphere-2026-5894
Preprint. Discussion started: 18 November 2026
© Author(s) 2026. CC BY 4.0 License.

To assess the potential contribution of biological INPs, heat-treatment analysis was conducted, as a loss of ice-nucleating activity upon heating can indicate heat-sensitive, proteinaceous material potentially originating from marine microorganisms. Figure 10 shows the heat-labile fraction of INPs after heat treatment at five different freezing temperatures from -12 °C to -22 °C for the different sample types evaluated in this study. The heat-labile fraction represents the relative decrease in INP activity after heating and is used to evaluate the contribution of thermally sensitive INPs. Values close to 1 indicate that most of the INP activity was destroyed by heating, whereas values close to 0 indicate that the INP activity was largely resistant to heat treatment.

The atmospheric filter samples displayed in Fig. 10(a) showed consistently high heat-labile fractions for the majority of the samples. For most of the cases, the values were above 0.8, indicating that a large fraction of the atmospheric INP population was sensitive to heating. Further, heat-labile fractions generally showed a decreasing trend with decreasing freezing temperature. This thermal sensitivity indicates that most INPs, and particularly those active at higher temperatures, were destroyed by heating, consistent with proteinaceous macromolecules which reduce their ice activity upon heating (Hartmann et al., 2021; Sze et al. 2023). Ambient filter samples collected over the MIZ and pack ice environments contained a higher fraction of heat-labile (biogenic) INPs than those collected over the open ocean water. This higher biological contribution to atmospheric INPs could originate from local natural sources connected to the presence of sea ice.

BSW exhibited the largest variability among the investigated sample types during heat test. This indicates that the seawater INP population was highly heterogeneous, containing both heat-sensitive and heat-resistant components. Prior Arctic and North Atlantic studies showed ubiquitous, often heat-sensitive INPs in BSW, together with evidence that sea spray efficiently transfers such INPs to the atmosphere, sometimes modulated by phytoplankton dynamics (DeMott et al. 2016; McCluskey et al. 2018; Irish et al. 2019; Creamean et al. 2019; Huang et al. 2021). However, the differences observed in heat-labile fractions between our atmospheric filter samples and the BSW samples already indicate that the ocean cannot be the only source for the atmospheric INPs we observed.

Melt-pond and surface sea ice samples also showed variable heat-labile fractions. Many samples have values above 0.5, suggesting that thermally sensitive INPs were common in these sea-ice associated environments. However, some melt-pond samples showed low heat-labile fractions, including values close to 0 at specific temperatures, indicating that heat-stable INPs also contributed to the observed ice-nucleating activity. This variability suggests that melt-pond and surface sea ice INP populations were compositionally mixed and likely influenced by changing biological activity, and exchange processes within the sea ice system. Previous studies indicated that melt-ponds and adjacent microhabitats host active biological communities and abundant organic macromolecules (Lee et al. 2012; Galgani et al. 2016; Hancke et al., 2022) that are frequently involved in high-temperature ice nucleation (Mavis et al., 2026). In this sense, melt-ponds provides a near-surface reservoir from which warm-onset, often proteinaceous INPs may be supplied to the boundary layer.

Fog water samples were characterized by predominantly high heat-labile fractions especially in the temperature range from -15 °C to -20 °C. These high heat-labile fractions point to a substantial biogenic contribution for INPs contained in fog. The resemblance in heat-lability of INPs between fog and atmospheric filter samples is larger

https://doi.org/10.5194/egusphere-2026-5894
Preprint. Discussion started: 18 November 2026
© Author(s) 2026. CC BY 4.0 License.

than that to other samples investigated herein, which is reasonable as INPs contained in fog originate from the atmosphere.

Overall, we found that heat-labile INPs were widespread across atmospheric, BSW, melt-pond, sea ice, and fog water samples. The consistently high heat-labile fractions in atmospheric filter and fog samples indicate that heat-sensitive INPs were especially present in the atmosphere. In contrast, the stronger variability observed in BSW and melt-pond and sea ice samples indicate the presence of heterogeneous INPs including biological heat-sensitive INPs and also heat-stable INPs. Previous Arctic studies also reported enhanced warm-temperature INPs in summer months (Wex et al., 2019). These INPs were linked to biological material rather than minerals (Sze et al., 2023), with contributions from both terrestrial and coastal marine environments (Wex et al., 2019; Hartmann et al., 2021; Creamean et al., 2022).

3.3.3 N_{INP} in comparison with literature

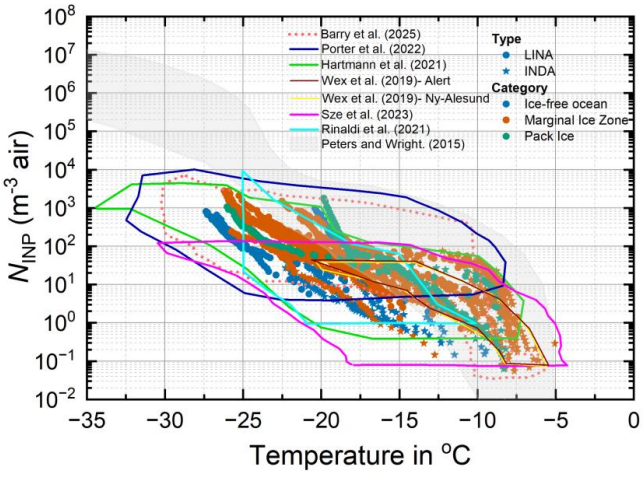


Figure-11: N_{INP} derived from atmospheric filter samples collected in this study compared with values reported in the literature. Barry et al. (2025), Porter et al. (2022), and Hartmann et al. (2021) shown Arctic summer measurements from the MOSAiC, MOCCHA, and PASCAL campaigns, respectively; Wex et al. (2019) shown summer measurements from Alert and Ny-Ålesund; Sze et al. (2023) shown summer measurements from Greenland; Rinaldi et al. (2021) shown spring and summer measurements from Ny-Ålesund; and Peters and Wright (2025) shown measurements from mid-latitude precipitation samples.

Figure 11 compares N_{INP} derived from atmospheric filter samples during this study with previous atmospheric INP studies. For this comparison it is important to keep in mind that upper and lower measurement limits of the separate studies differ. The gray-shaded area shows N_{INP} reported from mid-latitude precipitation samples by Petters and Wright (2015). More than 95% of the atmospheric filter-derived N_{INP} values from the present study are of similar magnitude to this range at higher temperatures, especially above ~ -20°C. It is remarkable that the abundance of warm-temperature INPs in our samples is broadly consistent with midlatitude observations by Petters and Wright (2015). However, the cold temperature INP population is less abundant.

https://doi.org/10.5194/egusphere-2026-5894
Preprint. Discussion started: 18 November 2026
© Author(s) 2026. CC BY 4.0 License.

In comparison with N_{INP} obtained from other Arctic studies, some differences are observed. The most striking difference concerns higher concentrations observed during the MOSAiC ship expedition in the central Arctic during summer (Barry et al., 2025) and during the summertime MOCCHA campaign at the North Pole (Porter et al., 2022). In the temperature range from roughly -10°C to -20°C, literature data exceed our maximum values by up to a factor of 50. At the same time, concentrations lower than ours were observed from ship measurements carried out in the European Arctic (Hartmann et al., 2021), from measurements at Greenland during summer (Sze et al., 2023), and from measurements in the Arctic during summer on Ny-Ålesund (Rinaldi et al., 2021), with a difference of less than one order of magnitude. Measurements done at Alert and Ny-Ålesund in the Arctic summer by Wex et al. (2019) cover a smaller range compared to ours. These differences may arise from rather limited numbers of samples examined in most studies, including ours, such that not all possible conditions are observed. Discovering reasons for these differences will have to go hand in hand with determining sources of INPs in future studies.

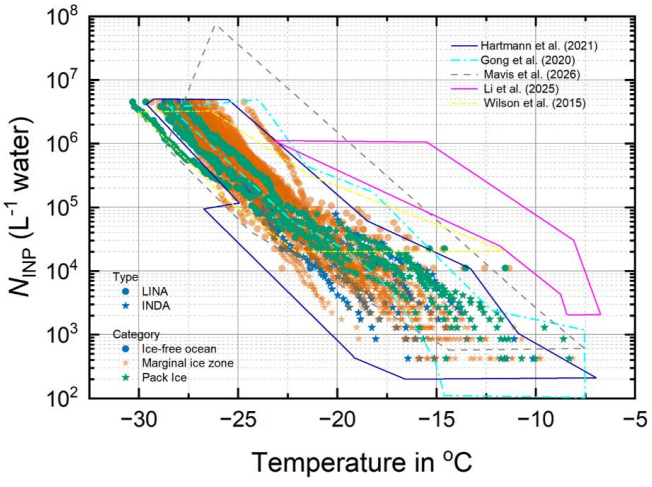


Figure-12: N_{INP} derived from the BSW samples in this study in comparison with the literature. Hartmann et al. (2021) represents Arctic summer, Gong et al represents Cabo Verde, Mavis et al. (2026) represents summer Arctic, Li et al. (2025) represents Eurasian Arctic, and Wilson et al. (2015) represents Arctic summer.

Figure 12 shows the INP concentrations derived from BSW samples collected during this study and compares them with previously reported N_{INP} datasets. The comparison with previous studies shows that our values for N_{INP} in BSW overlap strongly with the broad range of earlier observations in the Arctic by Wilson et al. (2015), Hartmann et al. (2021) and Mavis et al. (2026). There is also agreement with measurements made for sea water samples at Cabo Verde (Gong et al., 2020), which is striking considering that quite different conditions may be expected in the equatorial Atlantic Ocean, compared to the Arctic. However, it is noted that the INP concentrations in BSW in this study are lower in comparison to values from three samples collected in the Eurasian Arctic reported by Li et al. (2025). But these samples were all sampled explicitly in coastal regions, which may show elevated INP concentrations (Wex et al., 2019), and in a region that was highlighted by Porter et al. (2022) as an Arctic region showing a particularly strong source of biogenic INPs. Therefore, similarities notwithstanding, the

https://doi.org/10.5194/egusphere-2026-5894
Preprint. Discussion started: 18 November 2026
© Author(s) 2026. CC BY 4.0 License.

observed differences point at a heterogeneity of marine N_{INP} which may modulate atmospheric INP concentrations as well.

The literature datasets also show substantial variability, emphasizing that seawater INP concentrations differ strongly among regions, seasons, and sampling environments. These differences may arise from factors such as variations in biological productivity, proximity to sea ice, and meltwater influence, as already Irish et al. (2017) connected high INP concentrations in Arctic Ocean waters to melting sea ice. Therefore, the comparison shown in Fig. 12 should be interpreted as an assessment of broad consistency rather than a direct one to one comparison.

Both melt-pond and surface sea ice samples showed substantial variability, spanning several orders of magnitude across the measured temperature range (Fig. 13). The observed concentrations largely fall within the range reported by Mavis et al. (2026), indicating that the present data are broadly consistent with previous measurements from sea-ice-influenced environments. Melt-pond and surface snow/ice samples showed overlapping concentration ranges, implying that both environments contained comparable INP populations, likely influenced by shared source material and exchange processes within the sea-ice system.

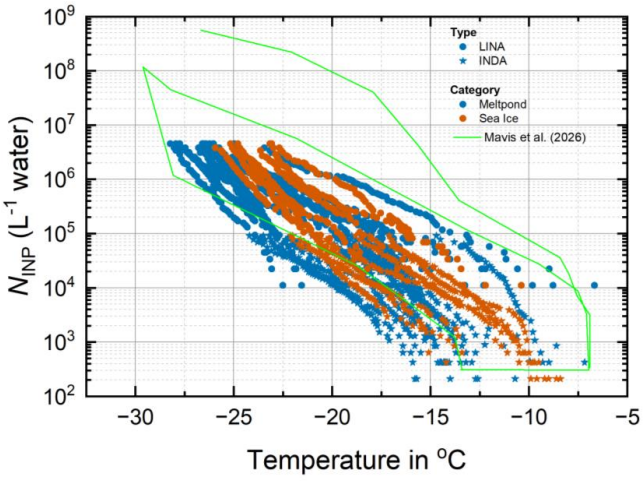


Figure-13: N_{INP} derived from the melt-pond and surface sea ice samples in comparison with the study by Mavis et al. (2026) in the Arctic. The extra green line specifically indicates a single measurement with high INP concentrations from the study by Mavis et al. (2026). This is added as a separate line to avoid giving a false impression.

Next, in Figure. 14, INP concentrations derived from fog water samples are compared with previously reported values from Arctic marine environments (Hartmann et al., 2021; Li et al., 2025), fog water measurements from the east coast of Nova Scotia, Canada (Schnell., 1977), and additionally with cloud water from the Cabo Verde region (Gong et al., 2020) and with values obtained at the Puy-de-Dôme atmospheric station in France (Joly et al., 2014). Overall, the present fog water INP concentrations fall within the broad range reported in earlier marine and Arctic studies, indicating that the observed concentrations are consistent with previously documented INP levels in marine-influenced cloud and fog water. The strongest overlap occurs with the ranges reported by

https://doi.org/10.5194/egusphere-2026-5894
Preprint. Discussion started: 18 November 2026
© Author(s) 2026. CC BY 4.0 License.

Hartmann et al. (2021), Li et al. (2025), Schnell (1977) and even with Gong et al. (2020) who measured in a tropical marine environment. However, the fog water INP concentrations measured in this study are generally lower than the data reported by Joly et al. (2014) from the terrestrial station of Puy-de-Dôme in France. This difference may reflect contrasting source environments, with the Puy-de-Dôme site being more strongly influenced by terrestrial aerosol sources, whereas the present samples were collected in a marine Arctic environment. Despite these differences in concentration level, the occurrence of freezing activity at temperatures warmer than approximately -10 °C in several data sets points to the presence of highly ice-active material. Such warm-temperature activity is generally consistent with contributions from biological or organic macromolecular INPs, although the exact source and composition may differ among regions (Hartmann et al., 2025). The overlap with previous marine observations suggests that fog in the Arctic marine boundary layer can contain INP populations comparable to those observed in other marine cloud and fog systems. At the same time, the lower concentrations relative to the Puy-de-Dôme dataset highlight the importance of regional source conditions and aerosol history in controlling INP abundance in cloud and fog water.

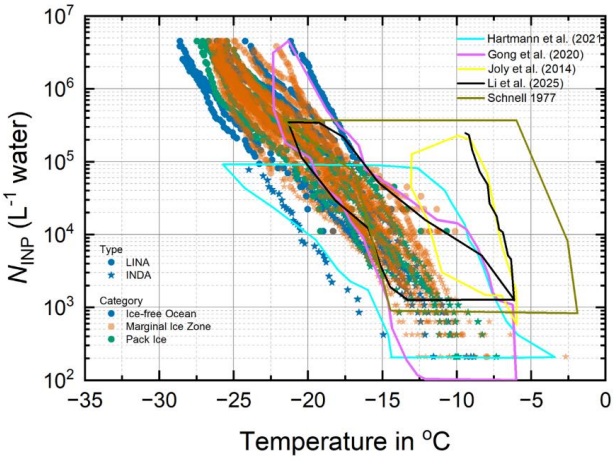


Figure-14: INP concentration derived from fog water samples in comparison with previous studies. Hartmann et al. (2021) represents measurements from Arctic summer, Gong et al. (2020) represents measurements from Cabo Verde islands, Joly et al. (2014) represents measurements from Puy de Dôme in France, Li et al. (2025) represents measurements from Eurasian Arctic, and Shnell et al. (1977) represents measurements from east-coast of Nova Scotia in Canada.

3.3.4 Sea spray derived INPs

To evaluate the potential contribution of oceanic emitted particles to atmospheric INP concentrations, sea spray aerosol derived INP concentrations were evaluated from INP concentrations measured for BSW (N_{INP}^{BSW}).

The sea spray derived INP concentrations in air ($N_{INP}^{sea\ spray}$) are calculated as,

$$N_{INP}^{sea\ spray} = \frac{Na_{mass,air}^{+}}{Na_{mass,BSW}^{+}} N_{INP}^{BSW}$$

https://doi.org/10.5194/egusphere-2026-5894
Preprint. Discussion started: 18 November 2026
© Author(s) 2026. CC BY 4.0 License.

where $Na^{+}_{mass,air}$ represents the mass concentrations of Na^{+} in the atmospheric INP filters evaluated as shown in Fig. S6, and $Na^{+}_{mass,BSW}$ represents the mass of Na^{+} in the BSW samples, respectively. $Na^{+}_{mass,BSW}$ seawater was calculated based on the salinity measurements of BSW. Based on the rule of proportion, i.e., assuming that Na^{+} and INPs occur in similar fractions in BSW and in atmospheric particles originating from sea spray generation, atmospheric INP concentrations were derived based on INP concentrations measured per unit volume of BSW. This provides an estimate of the INP concentration that could be expected in air if the observed seawater INPs were transferred to the atmosphere through sea spray production similarly to the transfer of NaCl (Hartmann et al. 2021; Gong et al., 2020; Irish et al., 2019).

The estimated $N_{INP}^{sea\ spray}$ are shown in Fig. 15 together with N_{INP} measured in the atmospheric filter samples in this study. The estimated sea spray derived N_{INP} are substantially lower than N_{INP} measured directly from the atmospheric filter samples by roughly two to three orders of magnitude. This large difference indicates that direct transfer of BSW INPs through sea spray, as estimated using the adopted approach, cannot explain the atmospheric INP concentrations observed during this study, unless strong enrichment in INPs during sea to air transfer is assumed.

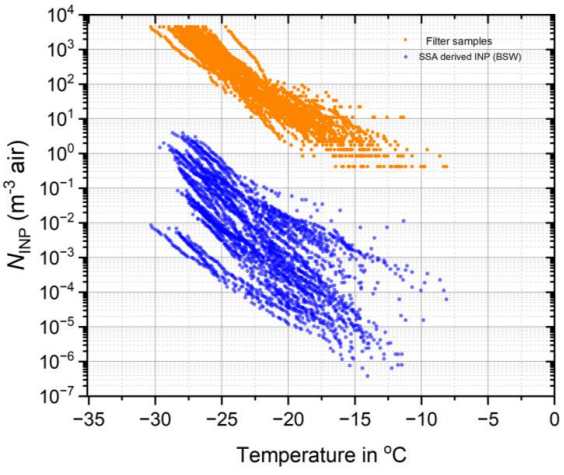


Figure-15: Sea spray derived N_{INP} derived from BSW samples (blue symbols). The orange symbols represent the N_{INP} directly derived from the atmospheric filter samples.

Similar observations were found by Hartmann et al. (2021) and Gong et al. (2020), who also used the similar approach. And, like us, they did infer atmospheric INP concentrations from INP concentrations of BSW, but also from the sea surface microlayer. For both cases, derived $N_{INP}^{sea\ spray}$ were substantially lower than ambient airborne INP concentrations, also by several orders of magnitude, as in this study. Also, Irish et al. (2019) examined N_{INP} in the Canadian Arctic marine boundary layer, together with an aerosol characterization. By deriving the surface area for both sea spray aerosol and mineral dust, they suggested that sea spray aerosol was a less important contributor to atmospheric INPs compared to mineral dust. All of these results suggest that BSW is as a reservoir of INPs, but the estimated sea spray contribution alone is insufficient to explain the measured atmospheric INP concentrations.

https://doi.org/10.5194/egusphere-2026-5894
Preprint. Discussion started: 18 November 2026
© Author(s) 2026. CC BY 4.0 License.

It should be mentioned that we did not investigate sea surface microlayer samples in this study. However, past studies examining N_{INP} from both, BSW and the sea surface microlayer often did not find a pronounced difference between these two (Hartmann et al., 2021; Gong et al., 2020; Li et al., 2025). Therefore, the large discrepancy between atmospheric N_{INP} and estimated INP concentrations from sea spray highlights the need to better constrain the transfer efficiency and enrichment of marine INPs during aerosolization.

3.3.5 Surface atmosphere exchange of aerosol particles and INP sources: 2 case studies

The preceding sections showed that N_{INP} in atmospheric filter samples, BSW, melt-ponds, sea ice, and fog water were highly variable. Highly ice-active and heat-labile INPs as found in the atmosphere and in fog water were not observed in the other samples to the same extent. Also, the comparison between measured atmospheric N_{INP} and sea spray derived INP concentrations indicated that BSW aerosolization alone could not explain the observed atmospheric INP concentrations without substantial enrichment during transfer of INPs to the aerosol phase. To further investigate whether local surface emissions could contribute to the atmospheric INP population, aerosol particle flux measurements were examined together with INP spectra for these cases. It should, however, be mentioned up front, that particle flux measurements are based on measured number concentrations of all particles, of which INPs are only a minor fraction (far below one per million), and that INPs can also be expected to have different sources than the majority of all other particles.

The vertical particle concentration profiles provide information on the direction of near-surface aerosol exchange. Assuming flux-gradient similarity, a decrease in particle number concentration with increasing measurement height indicates net upward transport and therefore net particle emission from the surface. In contrast, an increase in particle concentration with height indicates net downward transport and net deposition to the surface. Open water and open leads are expected to act as local sources of aerosol particles through wind driven sea spray production and bubble bursting, whereas snow and ice-covered surfaces can act as sinks for atmospheric particles through deposition. This conceptual framework was developed from previous Arctic observations showing enhanced particle emissions near open leads and deposition over closed ice or snow surfaces (Held et al. 2011; Mathes et al., 2025).

Figures 16(a) and 16(b) shows the case studies of two contrasting exchange regimes. On August 10 (Fig 16(a)), the vertical profile was measured over a wide lead with extensive open-water influence. This profile is based on six height levels between 46 cm and 760 cm above sea level (a.s.l). The profile showed decreasing particle concentration with height, corresponding to a net emission flux of 2.2×10^6 m^{-2} s^{-1}. The mean particle concentration was approximately 607 cm^{-3}, and the friction velocity derived from a mean wind speed of 2.3 m s^{-1} was 0.15 m s^{-1}. This case represents an active local emission regime, most likely associated with open-water particle production (Norris et al., 2011). By contrast, the profile measured on 29th of July over ice floes showed increasing particle concentration with height and therefore net deposition, with an estimated flux of -0.054×10^6 m^{-2} s^{-1}. This profile is based on eight height levels between 64 cm and 1100 cm a.s.l. The mean particle concentration was approximately 10 cm^{-3}, and the friction velocity was 0.16 m s^{-1} for a mean wind speed of 4.3 m s^{-1}. The contrast between these two profiles supports the above given interpretation that open leads can provide

https://doi.org/10.5194/egusphere-2026-5894
Preprint. Discussion started: 18 November 2026
© Author(s) 2026. CC BY 4.0 License.

local particle sources, whereas consolidated ice surfaces more commonly act as particle sinks (Held et al., 2011; Mathes et al., 2025).

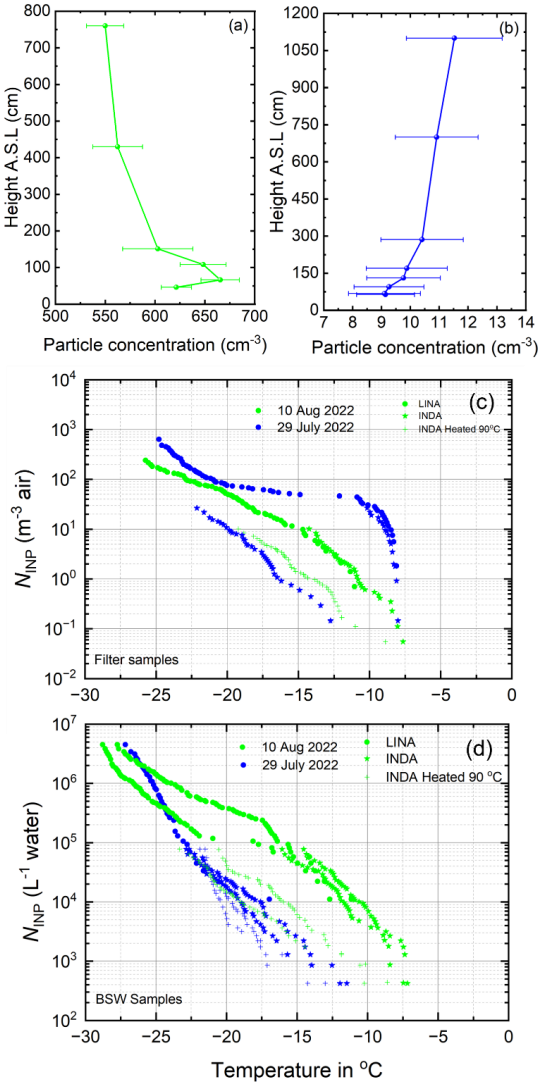


Figure 16: a) Profile indicating net emission from 10 August, and b) profile indicating net deposition from the 29 July. Error bars indicate the standard deviation of particle number concentration at each height level. INP concentration derived from (c) the airborne filter samples, and (d) the corresponding BSW samples.

The possible link between particle exchange and N_{INP} was assessed by comparing INP spectra measured during these selected emission and deposition cases. On 10th August, the strong net particle emission over ice-free ocean coincided with the presence of only comparably few warm-temperature atmospheric INPs. These INPs were clearly reduced after heat treatment, indicating the presence of heat-labile INPs. The corresponding INPs in BSW

https://doi.org/10.5194/egusphere-2026-5894
Preprint. Discussion started: 18 November 2026
© Author(s) 2026. CC BY 4.0 License.

showed a roughly comparable heat sensitivity, making it possible that at least part of the atmospheric INP population may have originated from local marine biological material. This interpretation is consistent with a mechanism in which bubble bursting or sea spray production transfers organic or biological ice-active material from the ocean surface to the atmosphere (Norris et al., 2011; DeMott et al., 2016). Marine organic macromolecules, exudates from microorganisms, and other biogenic material associated with seawater or the sea surface microlayer have been shown in previous studies to contribute to ice nucleation activity, particularly at relatively warm sub-zero temperatures (Wilson et al., 2015; Irish et al., 2017; Chance et al., 2018; Ickes et al., 2020).

In contrast, the deposition case on 29th of July in the MIZ showed a different behavior. Although the atmospheric INP spectrum exhibited enhanced warm-temperature ice activity of heat-labile INPs, INPs in the collocated BSW sample did neither show such an enhanced ice activity nor show a corresponding heat-labile signal. In fact, as can be seen in Fig. 16 (c-d), none of the BSW samples had enhanced N_{INP} similar to that seen in some atmospheric INP spectra. This mismatch suggests that the warm-temperature INPs observed in the atmosphere that led to enhanced concentrations above ~ -15°C were not directly produced from local seawater. Instead, they may have been transported from upwind sources, likely including terrestrial sources, before being deposited over the ice-covered surface. Such a decoupling between atmospheric INPs and seawater INPs highlights the complexity of source attribution in the Arctic marine boundary layer, where local emissions, long-range transport, and deposition occur simultaneously or sequentially. Further, the airmass trajectories during this period were traversing significantly through pack ice, contrary to the case on 10th August, when the airmass trajectories were mostly traversing through open ocean waters, only.

Taken together, these case studies demonstrate that the sign of the aerosol particle flux can be useful for interpreting atmospheric INP spectra. During open-water emission conditions, the co-occurrence of upward particle fluxes and heat-labile INPs in both the atmosphere and the seawater supports a local marine contribution to the atmospheric INP population. During deposition conditions over ice floes, the presence of highly ice-active atmospheric INPs without a corresponding seawater signal suggests that the INPs were more likely advected from non-local sources and subsequently deposited to the surface. These observations are consistent with earlier studies indicating that Arctic INPs can originate from both marine and non-marine sources, with biological or proteinaceous INPs often contributing at higher freezing temperatures, and mineral or refractory components becoming more important at lower temperatures.

Overall, this new approach of combined flux and INP measurements can provide evidence for two contrasting regimes: a local marine emission regime associated with ice-free ocean and heat-labile INPs, and a deposition regime in which atmospheric INPs are decoupled from the immediate surface reservoir. While these case studies do not provide a complete quantitative closure between surface INP reservoirs and atmospheric INP concentrations, they demonstrate that surface-atmosphere exchange measurements can substantially improve the interpretation of INP source pathways. Future work combining INP spectra, aerosol fluxes, chemical composition, biological tracers (particles or DNA analysis), airmass history, and direct measurements of sea spray enrichment will be essential for constraining the efficiency with which marine and sea ice associated INPs are transferred to the Arctic atmosphere.

https://doi.org/10.5194/egusphere-2026-5894
Preprint. Discussion started: 18 November 2026
© Author(s) 2026. CC BY 4.0 License.

4. Summary and Conclusion

During the ATWAICE expedition aboard RV *Polarstern*, we investigated how surface conditions, transport, meteorology, and atmospheric processing modulates aerosol particle size distribution, optical properties, chemical composition of aerosols and fog, and ice nucleating particles across ice-free ocean, MIZ, and pack ice in the Arctic. Our findings provide critical insights to help constrain the interactions between aerosols and climate in the Arctic. The results reveal a highly dynamic Arctic marine boundary layer in which neither aerosol abundance and composition nor INP activity can be attributed to a single dominant source or process.

The transition from ice-free ocean to pack ice was associated with systematic changes in particle size distributions and chemical composition. Aerosol particle number size distributions were persistently dominated by Aitken mode particles and were distinctly multimodal, with total number concentrations ranging below 10 cm^{-3} to more than 4000 cm^{-3} during specific episodic transport of particles during warm airmass intrusions or via new particle formation processes. Chemical composition varied systematically across the three surface regimes. Aerosols over the ice-free ocean had a strong sea-salt signature, whereas samples from the MIZ and pack ice were increasingly enriched in OM and SO_4^{2-}. Fog water retained a sea-salt contribution in all regimes, but DOM became dominant over the MIZ and pack ice. Correlation patterns indicate that primary sea spray coexisted with secondary products formed through marine biogenic sulfur and organic-precursor oxidation, with further modification during atmospheric transport and fog or cloud processing.

Investigation of the INP properties across multiple environmental compartments including ambient air, BSW, melt-ponds, sea ice samples, and fog water show that, N_{INP} were highly variable across all compartments, but with clear differences in magnitude, temperature dependence, and heat sensitivity among sample types. Melt-ponds and sea ice frequently contained more ice-active material than BSW, identifying cryospheric surface reservoirs as potentially important contributors. Atmospheric INP concentrations were generally enhanced in the MIZ and pack ice, and substantial numbers of INPs active at temperatures as warm as -10 °C were found only in atmospheric filter samples from these environments. Fog water INP concentrations were broadly comparable to those in melt-ponds and sea ice but showed a lower abundance of the most ice-active INPs than some atmospheric samples. This difference is consistent with preferential activation and subsequent removal of highly ice-active particles during fog processing, although additional observations are required to confirm this mechanism.

Heat-treatment of the samples revealed that heat-labile INPs were widespread across the investigated compartments. Ambient air and fog water samples were characterized by consistently high heat-labile fractions, particularly at higher temperatures, indicating that thermally sensitive, likely biological or proteinaceous material contributed substantially to the observed ice-nucleating activity. In contrast, BSW, melt-pond, and sea ice samples showed more heterogeneous heat responses, with both heat-labile and heat-stable INPs contributing to freezing activity. These results suggest that biological INPs are important in the Arctic marine atmosphere. Estimated INP emissions from direct aerosolization of BSW were two to three orders of magnitude lower than measured atmospheric concentrations. Consequently, direct transfer from BSW cannot explain the atmospheric INP burden without substantial enrichment during sea-to-air transfer, modification or production of ice-active material in surface reservoirs, or contributions from additional local and transported sources.

https://doi.org/10.5194/egusphere-2026-5894
Preprint. Discussion started: 18 November 2026
© Author(s) 2026. CC BY 4.0 License.

Case studies combining vertical measurements of aerosol particles above the sea level and INP spectra provided additional insight into possible surface atmosphere exchange pathways. Under ice-free ocean emission conditions, upward particle fluxes coincided with comparable INP spectra in both atmosphere and corresponding BSW sample, supporting a possible local marine contribution. In contrast, under particle deposition conditions over ice floes, enhanced high-temperature atmospheric INPs were not present in the corresponding BSW, suggesting that these INPs more likely originated from advection from non-local sources. These case studies demonstrate that particle flux measurements can provide valuable context for interpreting atmospheric INP observations, even though they do not yet provide quantitative closure between surface reservoirs and airborne INP concentrations.

Our findings show that Arctic INP abundance and composition cannot be explained by a single local source. Instead, the observed INP population reflects variable coupling among marine aerosol production, sea-ice associated surface reservoirs, fog water INPs, and long range transported aerosols. Heat-labile, very likely biological INPs appear to play an important role at higher freezing temperatures, particularly in atmospheric aerosol and fog water, while heat-stable components also contribute to selected surface reservoirs and at lower temperatures. Future work should combine INP spectra with direct SML sampling, analysis of aerosol chemistry and biological tracers through DNA analysis, sea spray enrichment measurements, and airmass histories to better quantify the pathways by which marine and sea ice associated INPs are transferred to the Arctic atmosphere.

Acknowledgements

We gratefully acknowledge the funding by the German Research Foundation, DFG grants WE 2757/6-1 and HE 5214/10-1. We gratefully acknowledge the support by Deutsche Forschungsgemeinschaft through the Transregional Collaborative Research Centre TRR-172 “ArctiC Amplification: Climate Relevant Atmospheric and SurfaCe Processes, and Feedback Mechanisms (AC)^3” (grant 268020496). We thank everyone involved in the expedition of the research vessel Polarstern during ATWAICE in 2022 (Grant No. AWI_PS131_11 (Alfred-Wegener-Institut Helmholtz Zentrum für Polar-und Meeresforschung, 2017). We thank Dr. Holger Seibert, Kay Weinhold and Anja Schmidt from the Leibniz Institute for Tropospheric Research, Germany for the support during this study. We thank the Institute of Environmental Physics, University of Bremen, for the provision of the merged MODIS-AMSR2 sea-ice concentration data at https://data.seaice.uni-bremen.de/modis_amsr2 (last access: 15 October 2023). We acknowledge the use of Grammarly during the preparation of this paper.

Author contributions

BSA, HW, BW and AH conceptualized the study. BSA, SL, PO conducted onboard measurements in the RV *Polarstern*. BSA, TM, MvP and ThM carried out the analysis. AW, JR provided the radiometer and radiosonde datasets. BSA prepared the original draft of the manuscript. All co-authors contributed to the interpretation of the results as well as review and editing.

Data availability

The dataset is being uploaded to Pangaea.

Competing Interests

At least one of the (co-) authors is a member of the editorial board of Atmospheric Chemistry and Physics.

https://doi.org/10.5194/egusphere-2026-5894
Preprint. Discussion started: 18 November 2026
© Author(s) 2026. CC BY 4.0 License.

References:

AMAP, 2024. AMAP Arctic Climate Change Update 2024: Key Trends and Impacts. Arctic Monitoring and Assessment Programme (AMAP), Tromsø, Norway. https://doi.org/10.21352/fz60-s852

Abbatt, J. P. D., Leaitch, W. R., Aliabadi, A. A., Bertram, A. K., Blanchet, J.-P., Boivin-Rioux, A., Bozem, H., Burkart, J., Chang, R. Y. W., Charette, J., Chaubey, J. P., Christensen, R. J., Cirisan, A., Collins, D. B., Croft, B., Dionne, J., Evans, G. J., Fletcher, C. G., Galí, M., Ghahreman, R., Girard, E., Gong, W., Gosselin, M., Gourdal, M., Hanna, S. J., Hayashida, H., Herber, A. B., Hesaraki, S., Hoor, P., Huang, L., Hussherr, R., Irish, V. E., Keita, S. A., Kodros, J. K., Köllner, F., Kolonjari, F., Kunkel, D., Ladino, L. A., Law, K., Levasseur, M., Libois, Q., Liggio, J., Lizotte, M., Macdonald, K. M., Mahmood, R., Martin, R. V., Mason, R. H., Miller, L. A., Moravek, A., Mortenson, E., Mungall, E. L., Murphy, J. G., Namazi, M., Norman, A.-L., O'Neill, N. T., Pierce, J. R., Russell, L. M., Schneider, J., Schulz, H., Sharma, S., Si, M., Staebler, R. M., Steiner, N. S., Thomas, J. L., von Salzen, K., Wentzell, J. J. B., Willis, M. D., Wentworth, G. R., Xu, J.-W., and Yakobi-Hancock, J. D.: Overview paper: New insights into aerosol and climate in the Arctic, Atmos. Chem. Phys., 19, 2527–2560, https://doi.org/10.5194/acp-19-2527-2019, 2019.

Arun, B. S., Müller, T., Pöhlker, M. L., Held, A., Pöhlker, C., van Pinxteren, M., Yang, Y., Lüchtrath, S., Walbröl, A., Rückert, J. E., Oehlke, P., Merkel, M., and Wehner, B.: Microphysical properties and light absorption enhancement of refractory black carbon aerosols in the central Arctic marine boundary layer: Role of warm airmass intrusions on mixing state, Atmos. Chem. Phys., 26, 7287–7310, https://doi.org/10.5194/acp-26-7287-2026, 2026.

Barry, K. R., Hill, T. C. J., Kreidenweis, S. M., Demott, P. J., Tobo, Y., and Creamean, J. M.: Bioaerosols as indicators of central Arctic ice nucleating particle sources, Atmos. Chem. Phys., 25, 11919–11933, https://doi.org/10.5194/acp-25-11919-2025, 2025.

Bergin, M. H., Jaffrezo, J., Davidson, C. I., Dibb, J. E., Pandis, S. N., Hillamo, R., Maenhaut, W., Kuhns, H. D., and Makela, T.: The contributions of snow, fog, and dry deposition to the summer flux of anions and cations at Summit, Greenland, JOURNAL OF GEOPHYSICAL RESEARCH, VOL. 100, NO. D8, PAGES 16,275-16,288, https://doi.org/10.1029/95JD01267, 1995

Boyer, M., Aliaga, D., Pernov, J. B., Angot, H., Quéléver, L. L. J., Dada, L., Heutte, B., Dall'Osto, M., Beddows, D. C. S., Brasseur, Z., Beck, I., Bucci, S., Duetsch, M., Stohl, A., Laurila, T., Asmi, E., Massling, A., Thomas, D. C., Nøjgaard, J. K., Chan, T., Sharma, S., Tunved, P., Krejci, R., Hansson, H. C., Bianchi, F., Lehtipalo, K., Wiedensohler, A., Weinhold, K., Kulmala, M., Petäjä, T., Sipilä, M., Schmale, J., and Jokinen, T.: A full year of aerosol size distribution data from the central Arctic under an extreme positive Arctic Oscillation: insights from the Multidisciplinary drifting Observatory for the Study of Arctic Climate (MOSAiC) expedition, Atmos. Chem. Phys., 23, 389–415, https://doi.org/10.5194/acp-23-389-2023, 2023.

Burrows, S. M., McCluskey, C. S., Cornwell, G., Steinke, I., Zhang, K., Zhao, B., Zawadowicz, M., Raman, A., Kulkarni, G., China, S., Zelenyuk, A., and DeMott, P. J.: Ice-Nucleating Particles That Impact Clouds and Climate: Observational and Modeling Research Needs, https://doi.org/10.1029/2021RG000745, 1 June 2022.

Cavalli, F., Viana, M., Yttri, K. E., Genberg, J., and Putaud, J.-P.: Atmospheric Measurement Techniques Toward a standardised thermal-optical protocol for measuring atmospheric organic and elemental carbon: the EUSAAR protocol, Atmos. Meas. Tech, 79–89 pp., https://doi.org/10.5194/amt-3-79-2010, 2010.

Chance, R. J., Hamilton, J. F., Carpenter, L. J., Hackenberg, S. C., Andrews, S. J., and Wilson, T. W.: Water-Soluble Organic Composition of the Arctic Sea Surface Microlayer and Association with Ice Nucleation Ability, Environ. Sci. Technol., 52, 1817–1826, https://doi.org/10.1021/acs.est.7b04072, 2018.

Chang, R. Y. W., Leck, C., Graus, M., Müller, M., Paatero, J., Burkhart, J. F., Stohl, A., Orr, L. H., Hayden, K., Li, S. M., Hansel, A., Tjernström, M., Leaitch, W. R., and Abbatt, J. P. D.: Aerosol composition and sources in the central Arctic Ocean during ASCOS, Atmos. Chem. Phys., 11, 10619–10636, https://doi.org/10.5194/acp-11-10619-2011, 2011.

Cohen, J., Zhang, X., Francis, J., Jung, T., Kwok, R., Overland, J., Ballinger, T. J., Bhatt, U. S., Chen, H. W., Coumou, D., Feldstein, S., Gu, H., Handorf, D., Henderson, G., Ionita, M., Kretschmer, M., Laliberte, F., Lee, S., Linderholm, H. W., Maslowski, W., Peings, Y., Pfeiffer, K., Rigor, I., Semmler, T., Stroeve, J., Taylor, P. C.,

https://doi.org/10.5194/egusphere-2026-5894
Preprint. Discussion started: 18 November 2026
© Author(s) 2026. CC BY 4.0 License.

Vavrus, S., Vihma, T., Wang, S., Wendisch, M., Wu, Y., and Yoon, J.: Divergent consensuses on Arctic amplification influence on midlatitude severe winter weather, https://doi.org/10.1038/s41558-019-0662-y, 1 January 2020.

Creamean, J. M., Cross, J. N., Pickart, R., McRaven, L., Lin, P., Pacini, A., Hanlon, R., Schmale, D. G., Ceniceros, J., Aydell, T., Colombi, N., Bolger, E., and DeMott, P. J.: Ice Nucleating Particles Carried From Below a Phytoplankton Bloom to the Arctic Atmosphere, Geophys. Res. Lett., 46, 8572–8581, https://doi.org/10.1029/2019GL083039, 2019.

Creamean, J. M., Barry, K., Hill, T. C. J., Hume, C., DeMott, P. J., Shupe, M. D., Dahlke, S., Willmes, S., Schmale, J., Beck, I., Hoppe, C. J. M., Fong, A., Chamberlain, E., Bowman, J., Scharien, R., and Persson, O.: Annual cycle observations of aerosols capable of ice formation in central Arctic clouds, Nat. Commun., 13, https://doi.org/10.1038/s41467-022-31182-x, 2022.

De Leeuw, G., Andreas, E. L., Anguelova, M. D., Fairall, C. W., Lewis, E. R., O'Dowd, C., Schulz, M., and Schwartz, S. E.: Production flux of sea spray aerosol, Reviews of Geophysics, 49, https://doi.org/10.1029/2010RG000349, 2011.

DeMott, P. J., Hill, T. C. J., McCluskey, C. S., Prather, K. A., Collins, D. B., Sullivan, R. C., Ruppel, M. J., Mason, R. H., Irish, V. E., Lee, T., Hwang, C. Y., Rhee, T. S., Snider, J. R., McMeeking, G. R., Dhaniyala, S., Lewis, E. R., Wentzell, J. J. B., Abbatt, J., Lee, C., Sultana, C. M., Ault, A. P., Axson, J. L., Martinez, M. D., Venero, I., Santos-Figueroa, G., Stokes, M. D., Deane, G. B., Mayol-Bracero, O. L., Grassian, V. H., Bertram, T. H., Bertram, A. K., Moffett, B. F., and Franc, G. D.: Sea spray aerosol as a unique source of ice nucleating particles, Proc. Natl. Acad. Sci. U. S. A., 113, 5797–5803, https://doi.org/10.1073/pnas.1514034112, 2016.

Demoz, B. B., Collett, J. L., and Daube, B. C.: On the CaltechActive Strand Cloudwater Collectors, Atmos. Res., 41, 47–62, https://doi.org/10.1016/0169-8095(95)00044-5, 1996

Ervens, B., Turpin, B. J., and Weber, R. J.: Secondary organic aerosol formation in cloud droplets and aqueous particles (aqSOA): A review of laboratory, field and model studies, https://doi.org/10.5194/acp-11-11069-2011, 2011.

Galgani, L., Piontek, J., and Engel, A.: Biopolymers form a gelatinous microlayer at the air-sea interface when Arctic sea ice melts, Sci. Rep., 6, https://doi.org/10.1038/srep29465, 2016.

Galí, M., Lizotte, M., Kieber, D. J., Randelhoff, A., Hussherr, R., Xue, L., Dinasquet, J., Babin, M., Rehm, E., and Levasseur, M.: DMS emissions from the Arctic marginal ice zone, Elementa, 9, https://doi.org/10.1525/elementa.2020.00113, 2021.

Gierens, R., Kneifel, S., D. Shupe, M., Ebell, K., Maturilli, M., and Löhnert, U.: Low-level mixed-phase clouds in a complex Arctic environment, Atmos. Chem. Phys., 20, 3459–3481, https://doi.org/10.5194/acp-20-3459-2020, 2020.

Gogoi, M. M., Pandey, S. K., Arun, B. S., Nair, V. S., Thakur, R. C., Chaubey, J. P., Tiwari, A., Manoj, M. R., Kompalli, S. K., Vaishya, A., Prijith, S. S., Hegde, P., and Babu, S. S.: Long-term changes in aerosol radiative properties over Ny-Ålesund: Results from Indian scientific expeditions to the Arctic, Polar Sci., 30, https://doi.org/10.1016/j.polar.2021.100700, 2021.

Gong, X., Wex, H., van Pinxteren, M., Triesch, N., Wadinga Fomba, K., Lubitz, J., Stolle, C., Robinson, T. B., Müller, T., Herrmann, H., and Stratmann, F.: Characterization of aerosol particles at Cabo Verde close to sea level and at the cloud level-Part 2: Ice-nucleating particles in air, cloud and seawater, Atmos. Chem. Phys., 20, 1451–1468, https://doi.org/10.5194/acp-20-1451-2020, 2020.

Gratzl, J., Böhmländer, A., Pätsi, S., Pogner, C. E., Gorfer, M., Brus, D., Doulgeris, K. M., Wieland, F., Asmi, E., Saarto, A., Möhler, O., Stolzenburg, D., and Grothe, H.: Locally emitted fungal spores serve as high-temperature ice nucleating particles in the European sub-Arctic, Atmos. Chem. Phys., 25, 12007–12035, https://doi.org/10.5194/acp-25-12007-2025, 2025.

Grémillet, D. and Descamps, S.: Ecological impacts of climate change on Arctic marine megafauna, https://doi.org/10.1016/j.tree.2023.04.002, 1 August 2023.

https://doi.org/10.5194/egusphere-2026-5894
Preprint. Discussion started: 18 November 2026
© Author(s) 2026. CC BY 4.0 License.

Griesche, H. J., Engelmann, R., Radenz, M., Hofer, J., Althausen, D., Ansmann, A., Barry, K., Creamean, J., Jimenez, C., and Seifert, P.: Annual cycle of surface-coupling effects on Arctic mixed-phase clouds during MOSAiC, Atmos. Chem. Phys., 26, 7141–7163, https://doi.org/10.5194/acp-26-7141-2026, 2026.

Guy, H., Brooks, I. M., Turner, D. D., Cox, C. J., Rowe, P. M., Shupe, M. D., Walden, V. P., and Neely, R. R.: Observations of Fog-Aerosol Interactions Over Central Greenland, Journal of Geophysical Research: Atmospheres, 128, https://doi.org/10.1029/2023JD038718, 2023.

Hancke, K., Kristiansen, S., and Lund-Hansen, L. C.: Highly Productive Ice Algal Mats in Arctic Melt-ponds: Primary Production and Carbon Turnover, Front. Mar. Sci., 9, https://doi.org/10.3389/fmars.2022.841720, 2022.

Hartmann, M., Gong, X., Kecorius, S., van Pinxteren, M., Vogl, T., Welti, A., Wex, H., Zeppenfeld, S., Herrmann, H., Wiedensohler, A., and Stratmann, F.: Terrestrial or marine - indications towards the origin of ice-nucleating particles during melt season in the European Arctic up to 83.7gN, Atmos. Chem. Phys., 21, 11613–11636, https://doi.org/10.5194/acp-21-11613-2021, 2021.

Hartmann, S., Schrödner, R., Hassett, B. T., Hartmann, M., van Pinxteren, M., Fomba, K. W., Stratmann, F., Herrmann, H., Pöhlker, M., and Zeppenfeld, S.: Polysaccharides-Important Constituents of Ice-Nucleating Particles of Marine Origin, Environ. Sci. Technol., 59, 5098–5108, https://doi.org/10.1021/acs.est.4c08014, 2025.

He, P., Alexander, B., Kang, H., Jiang, B., Yu, X., Yue, F., and Xie, Z.: Isotopic Constraints on the Formation Mechanisms of Sulfate Aerosols in the Summer Arctic Marine Boundary Layer, Journal of Geophysical Research: Atmospheres, 127, https://doi.org/10.1029/2022JD036601, 2022.

Heintzenberg, J. and Leck, C.: The summer aerosol in the central Arctic 1991-2008: Did it change or not?, Atmos. Chem. Phys., 12, 3969–3983, https://doi.org/10.5194/acp-12-3969-2012, 2012.

Heintzenberg, J., Leck, C., and Tunved, P.: Potential source regions and processes of aerosol in the summer Arctic, Atmos. Chem. Phys., 15, 6487–6502, https://doi.org/10.5194/acp-15-6487-2015, 2015.

Held, A., Brooks, I. M., Leck, C., and Tjernström, M.: On the potential contribution of open lead particle emissions to the central Arctic aerosol concentration, Atmos. Chem. Phys., 11, 3093–3105, https://doi.org/10.5194/acp-11-3093-2011, 2011.

Heutte, B., Bergner, N., Angot, H., Pernov, J. B., Dada, L., Mirrielees, J. A., Beck, I., Baccarini, A., Boyer, M., Creamean, J. M., Daellenbach, K. R., El Haddad, I., Frey, M. M., Henning, S., Laurila, T., Moschos, V., Petäjä, T., Pratt, K. A., Quéléver, L. L. J., Shupe, M. D., Zieger, P., Jokinen, T., and Schmale, J.: Observations of high-time-resolution and size-resolved aerosol chemical composition and microphysics in the central Arctic: implications for climate-relevant particle properties, Atmos. Chem. Phys., 25, 2207–2241, https://doi.org/10.5194/acp-25-2207-2025, 2025a.

Heutte, B., Angot, H., Chen, G. I., Pernov, J. B., El Haddad, I., Dada, L., Daellenbach, K. R., Beck, I., Bergner, N., Bucci, S., Creamean, J. M., Kulmala, M., Laurila, T., Petäjä, T., Pratt, K. A., Prévôt, A. S. H., Quéléver, L. L. J., Zieger, P., Jokinen, T., and Schmale, J.: Sources and Composition of Organic Aerosols in the Central Arctic during Spring and Summer, Environ. Sci. Technol., 59, 21924–21940, https://doi.org/10.1021/acs.est.5c09788, 2025b.

Hill, T. C. J., Demott, P. J., Tobo, Y., Fröhlich-Nowoisky, J., Moffett, B. F., Franc, G. D., and Kreidenweis, S. M.: Sources of organic ice nucleating particles in soils, Atmos. Chem. Phys., 16, 7195–7211, https://doi.org/10.5194/acp-16-7195-2016, 2016.

Hsu, S. C., Liu, S. C., Kao, S. J., Jeng, W. L., Huang, Y. T., Tseng, C. M., Tsai, F., Tu, J. Y., and Yang, Y.: Water-soluble species in the marine aerosol from the northern South China Sea: High chloride depletion related to air pollution, Journal of Geophysical Research Atmospheres, 112, https://doi.org/10.1029/2007JD008844, 2007.

Huang, S., Hu, W., Chen, J., Wu, Z., Zhang, D., and Fu, P.: Overview of biological ice nucleating particles in the atmosphere, https://doi.org/10.1016/j.envint.2020.106197, 1 January 2021.

Ickes, L., Porter, G. C. E., Wagner, R., Adams, M. P., Bierbauer, S., Bertram, A. K., Bilde, M., Christiansen, S., Ekman, A. M. L., Gorokhova, E., Höhler, K., Kiselev, A. A., Leck, C., Möhler, O., Murray, B. J., Schiebel, T.,

https://doi.org/10.5194/egusphere-2026-5894
Preprint. Discussion started: 18 November 2026
© Author(s) 2026. CC BY 4.0 License.

Ullrich, R., and Salter, M. E.: The ice-nucleating activity of Arctic sea surface microlayer samples and marine algal cultures, Atmos. Chem. Phys., 20, 11089–11117, https://doi.org/10.5194/acp-20-11089-2020, 2020.

IPCC, 2019: IPCC Special Report on the Ocean and Cryosphere in a Changing Climate [H.-O. Pörtner, D.C. Roberts, V. Masson-Delmotte, P. Zhai, M. Tignor, E. Poloczanska, K. Mintenbeck, A. Alegría, M. Nicolai, A. Okem, J. Petzold, B. Rama, N.M. Weyer (eds.)]. Cambridge University Press, Cambridge, UK and New York, NY, USA, 755 pp. https://doi.org/10.1017/9781009157964.

IPCC, 2022: Climate Change 2022: Impacts, Adaptation and Vulnerability. Contribution of Working Group II to the Sixth Assessment Report of the Intergovernmental Panel on Climate Change [H.-O. Pörtner, D.C. Roberts, M. Tignor, E.S. Poloczanska, K. Mintenbeck, A. Alegría, M. Craig, S. Langs-dorf, S. Löschke, V. Möller, A. Okem, B. Rama (eds.)]. Cambridge University Press. Cambridge University Press, Cambridge, UK and New York, NY, USA, 3056 pp., doi:10.1017/9781009325844.

Irish, V. E., Elizondo, P., Chen, J., Choul, C., Charette, J., Lizotte, M., Ladino, L. A., Wilson, T. W., Gosselin, M., Murray, B. J., Polishchuk, E., Abbatt, J. P. D., Miller, L. A., and Bertram, A. K.: Ice-nucleating particles in Canadian Arctic sea-surface microlayer and bulk seawater, Atmos. Chem. Phys., 17, 10583–10595, https://doi.org/10.5194/acp-17-10583-2017, 2017.

Irish, V. E., Hanna, S. J., Xi, Y., Boyer, M., Polishchuk, E., Ahmed, M., Chen, J., Abbatt, J. P. D., Gosselin, M., Chang, R., Miller, L. A., and Bertram, A. K.: Revisiting properties and concentrations of ice-nucleating particles in the sea surface microlayer and bulk seawater in the Canadian Arctic during summer, Atmos. Chem. Phys., 19, 7775–7787, https://doi.org/10.5194/acp-19-7775-2019, 2019.

Joly, M., Amato, P., Deguillaume, L., Monier, M., Hoose, C., and Delort, A. M.: Quantification of ice nuclei active at near 0 °c temperatures in low-altitude clouds at the Puy de Dôme atmospheric station, Atmos. Chem. Phys., 14, 8185–8195, https://doi.org/10.5194/acp-14-8185-2014, 2014.

Jurányi, Z., Zanatta, M., Lund, M. T., Samset, B. H., Skeie, R. B., Sharma, S., Wendisch, M., and Herber, A.: Atmospheric concentrations of black carbon are substantially higher in spring than summer in the Arctic, Commun. Earth Environ., 4, https://doi.org/10.1038/s43247-023-00749-x, 2023.

Kanzow, T.: Berichte zur Polar- und Meeresforschung, Bericht Nr. 770/2023, https://doi.org/10.57738/BzPM_0770_2023, 2023.

Kecorius, S., Vogl, T., Paasonen, P., Lampilahti, J., Rothenberg, D., Wex, H., Zeppenfeld, S., van Pinxteren, M., Hartmann, M., Henning, S., Gong, X., Welti, A., Kulmala, M., Stratmann, F., Herrmann, H., and Wiedensohler, A.: New particle formation and its effect on cloud condensation nuclei abundance in the summer Arctic: A case study in the Fram Strait and Barents Sea, Atmos. Chem. Phys., 19, 14339–14364, https://doi.org/10.5194/acp-19-14339-2019, 2019.

Kecorius, S., Hoffmann, E. H., Tilgner, A., Barrientos-Velasco, C., van Pinxteren, M., Zeppenfeld, S., Vogl, T., Madueño, L., Lovrić, M., Wiedensohler, A., Kulmala, M., Paasonen, P., and Herrmann, H.: Rapid growth of Aitken-mode particles during Arctic summer by fog chemical processing and its implication, PNAS Nexus, 2, https://doi.org/10.1093/pnasnexus/pgad124, 2023.

Leck, C., Heintzenberg, J., Nygård, T., and Naakka, T.: Is the summer aerosol over the Arctic controlled by regional atmospheric circulation or ice conditions? Trends and future implications, Atmos. Chem. Phys., 25, 16775–16795, https://doi.org/10.5194/acp-25-16775-2025, 2025.

Lee, S. H., Stockwell, D. A., Joo, H. M., Son, Y. B., Kang, C. K., and Whitledge, T. E.: Phytoplankton production from melting ponds on Arctic sea ice, J. Geophys. Res. Oceans, 117, https://doi.org/10.1029/2011JC007717, 2012.

Legrand, M., Preunkert, S., Wolff, E., Weller, R., Jourdain, B., and Wagenbach, D.: Year-round records of bulk and size-segregated aerosol composition in central Antarctica (Concordia site) - Part 1: Fractionation of sea salt particles, Atmos. Chem. Phys., 17, 14039–14054, https://doi.org/10.5194/acp-17-14039-2017, 2017.

https://doi.org/10.5194/egusphere-2026-5894
Preprint. Discussion started: 18 November 2026
© Author(s) 2026. CC BY 4.0 License.

Leon-Marcos, A., van Pinxteren, M., Zeppenfeld, S., Zeising, M., Bracher, A., Oziel, L., Tegen, I., and Heinold, B.: Thirty years of arctic primary marine organic aerosols: patterns, seasonal dynamics, and trends (1990–2019), Atmos. Chem. Phys., 26, 1109–1144, https://doi.org/10.5194/acp-26-1109-2026, 2026.

Li, G., Welti, A., Thurnherr, I., Lohmann, U., and Kanji, Z. A.: Ice Nucleating Particle Concentrations over the Eurasian-Arctic seas, https://doi.org/10.5194/egusphere-2025-2798, 2025.

Li, J., Carlson, B. E., Yung, Y. L., Lv, D., Hansen, J., Penner, J. E., Liao, H., Ramaswamy, V., Kahn, R. A., Zhang, P., Dubovik, O., Ding, A., Lacis, A. A., Zhang, L., and Dong, Y.: Scattering and absorbing aerosols in the climate system, https://doi.org/10.1038/s43017-022-00296-7, 2022.

Ludwig, V., Spreen, G., and Pedersen, L. T.: Evaluation of a new merged sea-ice concentration dataset at 1 km resolution from thermal infrared and passive microwave satellite data in the arctic, Remote Sens. (Basel)., 12, 1–28, https://doi.org/10.3390/rs12193183, 2020.

Mathes, T., Guy, H., Prytherch, J., Kojoj, J., Brooks, I., Murto, S., Zieger, P., Wehner, B., Tjernström, M., and Held, A.: Particle flux-gradient relationships in the high Arctic: Emission and deposition patterns across three surface types, Atmos. Chem. Phys., 25, 8455–8474, https://doi.org/10.5194/acp-25-8455-2025, 2025.

Mavis, C. E., Vazquez, M., Bekemeier, C. A., Barry, K. R., Chamberlain, E. J., Schmale, J., Jokinen, T., Laurila, T., Shupe, M. D., Hoppe, C. J. M., Fong, A. A., Oggier, M., Ulfsbo, A., Balmonte, J. P., Bowman, J. S., Hill, T. C. J., DeMott, P. J., Kreidenweis, S. M., and Creamean, J. M.: Meltwater as a Local Source of Ice Nucleating Particles in the Central Arctic Summer, Geophys. Res. Lett., 53, https://doi.org/10.1029/2025GL118445, 2026.

McCluskey, C. S., Ovadnevaite, J., Rinaldi, M., Atkinson, J., Belosi, F., Ceburnis, D., Marullo, S., Hill, T. C. J., Lohmann, U., Kanji, Z. A., O'Dowd, C., Kreidenweis, S. M., and DeMott, P. J.: Marine and Terrestrial Organic Ice-Nucleating Particles in Pristine Marine to Continentally Influenced Northeast Atlantic Airmasses, Journal of Geophysical Research: Atmospheres, 123, 6196–6212, https://doi.org/10.1029/2017JD028033, 2018.

Millero, F. J. and Sohn, M. L.: Chemical Oceanography, CRC Press, Boca Raton, FL, 531 pp., ISBN 978-0-8493-8840-8, 1992.

Moallemi, A., Alberello, A., Thurnherr, I., Li, G., Kanji, Z. A., Bergamasco, F., Pohorsky, R., Nelli, F., Toffoli, A., and Schmale, J.: Links between atmospheric aerosols and sea state in the Arctic Ocean, Atmos. Environ., 338, https://doi.org/10.1016/j.atmosenv.2024.120844, 2024.

Morrison, H., De Boer, G., Feingold, G., Harrington, J., Shupe, M. D., and Sulia, K.: Resilience of persistent Arctic mixed-phase clouds, https://doi.org/10.1038/ngeo1332, January 2012., 2012.

Müller, T., Laborde, M., Kassell, G., and Wiedensohler, A.: Design and performance of a three-wavelength LED-based total scatter and backscatter integrating nephelometer, Atmos. Meas. Tech., 4, 1291–1303, https://doi.org/10.5194/amt-4-1291-2011, 2011.

Müller, K., Lehmann, S., van Pinxteren, D., Gnauk, T., Niedermeier, N., Wiedensohler, A., and Herrmann, H.: Particle characterization at the Cape Verde atmospheric observatory during the 2007 RHaMBLe intensive, Atmos. Chem. Phys., 10, 2709–2721, https://doi.org/10.5194/acp-10-2709-2010, 2010.

Nilsson, E. D. and Leck, C.: A pseudo-Lagrangian study of the sulfur budget in the remote Arctic marine boundary layer, 54, 213–230., DOI: 10.3402/tellusb.v54i3.16662, 2002.

Noone Kevin, B. J., Ogren, J. A., Hallberg, A., Heintzenberg, J., and Strom, J.: Changes in aerosol size-and phase distributions due to physical and chemical processes in fog, 489–504 pp., DOI: 10.3402/tellusb.v44i5.15563, 1992.

Norris, S. J., Brooks, I. M., De Leeuw, G., Sirevaag, A., Leck, C., Brooks, B. J., Birch, C. E., and Tjernström, M.: Measurements of bubble size spectra within leads in the Arctic summer pack ice, Ocean Science, 7, 129–139, https://doi.org/10.5194/os-7-129-2011, 2011.

Petters, M. D. and Wright, T. P.: Revisiting ice nucleation from precipitation samples, Geophys. Res. Lett., 42, 8758–8766, https://doi.org/10.1002/2015GL065733, 2015.

https://doi.org/10.5194/egusphere-2026-5894
Preprint. Discussion started: 18 November 2026
© Author(s) 2026. CC BY 4.0 License.

Pfeifer, S., Birmili, W., Schladitz, A., Müller, T., Nowak, A., and Wiedensohler, A.: A fast and easy-to-implement inversion algorithm for mobility particle size spectrometers considering particle number size distribution information outside of the detection range, Atmos. Meas. Tech., 7, 95–105, https://doi.org/10.5194/amt-7-95-2014, 2014.

Pilz, C., Cassano, J. J., de Boer, G., Kirbus, B., Lonardi, M., Pöhlker, M., Shupe, M. D., Siebert, H., Wendisch, M., and Wehner, B.: Tethered balloon measurements reveal enhanced aerosol occurrence aloft interacting with Arctic low-level clouds, Elementa, 12, https://doi.org/10.1525/elementa.2023.00120, 2024.

Pereira Freitas, G., Adachi, K., Conen, F., Heslin-Rees, D., Krejci, R., Tobo, Y., Yttri, K. E., and Zieger, P.: Regionally sourced bioaerosols drive high-temperature ice nucleating particles in the Arctic, Nature Communications , 14, https://doi.org/10.1038/s41467-023-41696-7, 2023.

Porter, G. C. E., Adams, M. P., Brooks, I. M., Ickes, L., Karlsson, L., Leck, C., Salter, M. E., Schmale, J., Siegel, K., Sikora, S. N. F., Tarn, M. D., Vüllers, J., Wernli, H., Zieger, P., Zinke, J., and Murray, B. J.: Highly Active Ice-Nucleating Particles at the Summer North Pole, Journal of Geophysical Research: Atmospheres, 127, https://doi.org/10.1029/2021JD036059, 2022.

Previdi, M., Smith, K. L., and Polvani, L. M.: Arctic amplification of climate change: A review of underlying mechanisms, https://doi.org/10.1088/1748-9326/ac1c29, 1 September 2021.

Pummer, B. G., Bauer, H., Bernardi, J., Bleicher, S., and Grothe, H.: Suspendable macromolecules are responsible for ice nucleation activity of birch and conifer pollen, Atmos. Chem. Phys., 12, 2541–2550, https://doi.org/10.5194/acp-12-2541-2012, 2012.

Rantanen, M., Karpechko, A. Y., Lipponen, A., Nordling, K., Hyvärinen, O., Ruosteenoja, K., Vihma, T., and Laaksonen, A.: The Arctic has warmed nearly four times faster than the globe since 1979, Commun. Earth Environ., 3, https://doi.org/10.1038/s43247-022-00498-3, 2022.

Rinaldi, M., Hiranuma, N., Santachiara, G., Mazzola, M., Mansour, K., Paglione, M., Rodriguez, C. A., Traversi, R., Becagli, S., Cappelletti, D., and Belosi, F.: Ice-nucleating particle concentration measurements from Ny-Ålesund during the Arctic spring-summer in 2018, Atmos. Chem. Phys., 21, 14725–14748, https://doi.org/10.5194/acp-21-14725-2021, 2021.

Schmale, J., Zieger, P., and Ekman, A. M. L.: Aerosols in current and future Arctic climate, Nat. Clim. Chang., 11, 95–105, https://doi.org/10.1038/s41558-020-00969-5, 2021.

Schnell, R. C.: Ice nuclei in seawater, fog water and marine air off the coast of Nova Scotia: Summer 1975, *J. Atmos. Sci.*, **34**, 1299–1305, https://doi.org/10.1175/1520-0469(1977)034<1299:INISFW>2.0.CO;2, 1977.

Schuur, E. A. G., Abbott, B. W., Commane, R., Ernakovich, J., Euskirchen, E., Hugelius, G., Grosse, G., Jones, M., Koven, C., Leshyk, V., Lawrence, D., Loranty, M. M., Mauritz, M., Olefeldt, D., Natali, S., Rodenhizer, H., Salmon, V., Schädel, C., Strauss, J., Treat, C., and Turetsky, M.: Annual Review of Environment and Resources Permafrost and Climate Change: Carbon Cycle Feedbacks From the Warming Arctic, 47, 343-371, https://doi.org/10.1146/annurev-environ-012220-011847, 2022.

Serreze, M. C. and Barry, R. G.: Processes and impacts of Arctic amplification: A research synthesis, Glob. Planet. Change, 77, 85–96, https://doi.org/10.1016/j.gloplacha.2011.03.004, 2011.

Shupe, M. D.: Clouds at arctic atmospheric observatories. Part II: Thermodynamic phase characteristics, J. Appl. Meteorol. Climatol., 50, 645–661, https://doi.org/10.1175/2010JAMC2468.1, 2011.

Simon, D. J., Hartmann, J., Schaefer, J., Zeppenfeld, S., Lüpkes, C., Hartmann, M., Wetzel, B., Heinold, B., Jurányi, Z., Schulz, A., Köhler, L., Jörss, A. M., Herber, A., Henning, S., Pöhlker, M. L., Roberts, G. C., and Stratmann, F.: Turbulent Aerosol Fluxes From Airborne Measurements Over the Arctic Ocean, Geophys. Res. Lett., 52, https://doi.org/10.1029/2025GL117094, 2025.

Singh, D. K., Kawamura, K., Fu, P., Kasukabe, H., Yanase, A., and Barrie, L. A.: Photochemical Processing of Inorganic and Organic Species in the Canadian High Arctic Aerosols: Impact of Ammonium Cation, Transition Metals, and Dicarboxylic Acids before and after Polar Sunrise at Alert, ACS Earth Space Chem., 5, 2865–2877, https://doi.org/10.1021/acsearthspacechem.1c00242, 2021.

https://doi.org/10.5194/egusphere-2026-5894
Preprint. Discussion started: 18 November 2026
© Author(s) 2026. CC BY 4.0 License.

Spreen, G., Kaleschke, L., and Heygster, G.: Sea ice remote sensing using AMSR-E 89-GHz channels, J. Geophys. Res. Oceans, 113, https://doi.org/10.1029/2005JC003384, 2008.

Stein, A. F., Draxler, R. R., Rolph, G. D., Stunder, B. J. B., Cohen, M. D., and Ngan, F.: Noaa's hysplit atmospheric transport and dispersion modeling system, https://doi.org/10.1175/BAMS-D-14-00110.1, 1 December 2015.

Stroeve, J. C., Serreze, M. C., Holland, M. M., Kay, J. E., Malanik, J., and Barrett, A. P.: The Arctic's rapidly shrinking sea ice cover: A research synthesis, Clim. Change, 110, 1005–1027, https://doi.org/10.1007/s10584-011-0101-1, 2012.

Sze, K. C. H., Wex, H., Hartmann, M., Skov, H., Massling, A., Villanueva, D., and Stratmann, F.: Ice-nucleating particles in northern Greenland: Annual cycles, biological contribution and parameterizations, Atmos. Chem. Phys., 23, 4741–4761, https://doi.org/10.5194/acp-23-4741-2023, 2023.

Tjernström, M., Leck, C., Birch, C. E., Bottenheim, J. W., Brooks, B. J., Brooks, I. M., Bäcklin, L., Chang, R. Y. W., De Leeuw, G., Di Liberto, L., De La Rosa, S., Granath, E., Graus, M., Hansel, A., Heintzenberg, J., Held, A., Hind, A., Johnston, P., Knulst, J., Martin, M., Matrai, P. A., Mauritsen, T., Müller, M., Norris, S. J., Orellana, M. V., Orsini, D. A., Paatero, J., Persson, P. O. G., Gao, Q., Rauschenberg, C., Ristovski, Z., Sedlar, J., Shupe, M. D., Sierau, B., Sirevaag, A., Sjogren, S., Stetzer, O., Swietlicki, E., Szczodrak, M., Vaattovaara, P., Wahlberg, N., Westberg, M., and Wheeler, C. R.: The Arctic Summer Cloud Ocean Study (ASCOS): Overview and experimental design, https://doi.org/10.5194/acp-14-2823-2014, 19 March 2014.

Vali, G.: Quantitative Evaluation of Experimental Results an the Heterogeneous Freezing Nucleation of Supercooled Liquids, J. Atmos. Sci., 28, 402–409, https://doi.org/10.1175/1520-0469(1971)028<0402:QEOERA>2.0.CO;2, 1971.

van Pinxteren, M., Barthel, S., Fomba, K. W., Müller, K., Von Tümpling, W., and Herrmann, H.: The influence of environmental drivers on the enrichment of organic carbon in the sea surface microlayer and in submicron aerosol particles – measurements from the Atlantic Ocean, Elementa, 5, https://doi.org/10.1525/elementa.225, 2017.

Wendisch, M., Brückner, M., Crewell, S., Ehrlich, A., Notholt, J., Lüpkes, C., Macke, A., Burrows, J. P., Rinke, A., Quaas, J., Maturilli, M., Schemann, V., Shupe, M. D., Akansu, E. F., Barrientos-Velasco, C., Bärfuss, K., Blechschmidt, A. M., Block, K., Bougoudis, I., Bozem, H., Böckmann, C., Bracher, A., Bresson, H., Bretschneider, L., Buschmann, M., Chechin, D. G., Chylik, J., Dahlke, S., Deneke, H., Dethloff, K., Donth, T., Dorn, W., Dupuy, R., Ebell, K., Egerer, U., Engelmann, R., Eppers, O., Gerdes, R., Gierens, R., Gorodetskaya, I. V., Gottschalk, M., Griesche, H., Gryanik, V. M., Handorf, D., Harm-Altstädter, B., Hartmann, J., Hartmann, M., Heinold, B., Herber, A., Herrmann, H., Heygster, G., Höschel, I., Hofmann, Z., Hölemann, J., Hünerbein, A., Jafariserajehlou, S., Jäkel, E., Jacobi, C., Janout, M., Jansen, F., Jourdan, O., Jurányi, Z., Kalesse-Los, H., Kanzow, T., Käthner, R., Kliesch, L. L., Klingebiel, M., Knudsen, E. M., Kovács, T., Körtke, W., Krampe, D., Kretzschmar, J., Kreyling, D., Kulla, B., Kunkel, D., Lampert, A., Lauer, M., Lelli, L., von Lerber, A., Linke, O., Löhnert, U., Lonardi, M., Losa, S. N., Losch, M., Maahn, M., Mech, M., Mei, L., Mertes, S., Metzner, E., Mewes, D., Michaelis, J., Mioche, G., Moser, M., Nakoudi, K., Neggers, R., Neuber, R., Nomokonova, T., Oelker, J., Papakonstantinou-Presvelou, I., Pätzold, F., Pefanis, V., Pohl, C., van Pinxteren, M., Radovan, A., Rhein, M., Rex, M., Richter, A., Risse, N., Ritter, C., Rostosky, P., Rozanov, V. V., Donoso, E. R., Garfias, P. S., Salzmann, M., Schacht, J., Schäfer, M., Schneider, J., Schnierstein, N., Seifert, P., Seo, S., Siebert, H., Soppa, M. A., Spreen, G., Stachlewska, I. S., Stapf, J., Stratmann, F., Tegen, I., Viceto, C., Voigt, C., Vountas, M., Walbröl, A., Walter, M., Wehner, B., Wex, H., Willmes, S., Zanatta, M., and Zeppenfeld, S.: Atmospheric and Surface Processes, and Feedback Mechanisms Determining Arctic Amplification, Bull. Am. Meteorol. Soc., 104, E208–E242, https://doi.org/10.1175/BAMS-D-21-0218.1, 2023.

Wex, H., Huang, L., Zhang, W., Hung, H., Traversi, R., Becagli, S., Sheesley, R. J., Moffett, C. E., Barrett, T. E., Bossi, R., Skov, H., Hünerbein, A., Lubitz, J., Löffler, M., Linke, O., Hartmann, M., Herenz, P., and Stratmann, F.: Annual variability of ice-nucleating particle concentrations at different Arctic locations, Atmos. Chem. Phys., 19, 5293–5311, https://doi.org/10.5194/acp-19-5293-2019, 2019.

Wiedensohler, A., Birmili, W., Nowak, A., Sonntag, A., Weinhold, K., Merkel, M., Wehner, B., Tuch, T., Pfeifer, S., Fiebig, M., Fjäraa, A. M., Asmi, E., Sellegri, K., Depuy, R., Venzac, H., Villani, P., Laj, P., Aalto, P., Ogren,

https://doi.org/10.5194/egusphere-2026-5894
Preprint. Discussion started: 18 November 2026
© Author(s) 2026. CC BY 4.0 License.

J. A., Swietlicki, E., Williams, P., Roldin, P., Quincey, P., Hüglin, C., Fierz-Schmidhauser, R., Gysel, M., Weingartner, E., Riccobono, F., Santos, S., Grüning, C., Faloon, K., Beddows, D., Harrison, R., Monahan, C., Jennings, S. G., O'Dowd, C. D., Marinoni, A., Horn, H. G., Keck, L., Jiang, J., Scheckman, J., McMurry, P. H., Deng, Z., Zhao, C. S., Moerman, M., Henzing, B., De Leeuw, G., Löschau, G., and Bastian, S.: Mobility particle size spectrometers: Harmonization of technical standards and data structure to facilitate high quality long-term observations of atmospheric particle number size distributions, Atmos. Meas. Tech., 5, 657–685, https://doi.org/10.5194/amt-5-657-2012, 2012.

Willis, M. D., Burkart, J., Thomas, J. L., Köllner, F., Schneider, J., Bozem, H., Hoor, P. M., Aliabadi, A. A., Schulz, H., Herber, A. B., Leaitch, W. R., and Abbatt, J. P. D.: Growth of nucleation mode particles in the summertime Arctic: A case study, Atmos. Chem. Phys., 16, 7663–7679, https://doi.org/10.5194/acp-16-7663-2016, 2016.

Wilson, T. W., Ladino, L. A., Alpert, P. A., Breckels, M. N., Brooks, I. M., Browse, J., Burrows, S. M., Carslaw, K. S., Huffman, J. A., Judd, C., Kilthau, W. P., Mason, R. H., McFiggans, G., Miller, L. A., Najera, J. J., Polishchuk, E., Rae, S., Schiller, C. L., Si, M., Temprado, J. V., Whale, T. F., Wong, J. P. S., Wurl, O., Yakobi-Hancock, J. D., Abbatt, J. P. D., Aller, J. Y., Bertram, A. K., Knopf, D. A., and Murray, B. J.: A marine biogenic source of atmospheric ice-nucleating particles, Nature, 525, 234–238, https://doi.org/10.1038/nature14986, 2015.

Zeppenfeld, S., van Pinxteren, M., van Pinxteren, D., Wex, H., Berdalet, E., Vaqué, D., Dall'Osto, M., and Herrmann, H.: Aerosol Marine Primary Carbohydrates and Atmospheric Transformation in the Western Antarctic Peninsula, ACS Earth Space Chem., 5, 1032–1047, https://doi.org/10.1021/acsearthspacechem.0c00351, 2021.

Zeppenfeld, S., van Pinxteren, M., Hartmann, M., Zeising, M., Bracher, A., and Herrmann, H.: Marine carbohydrates in Arctic aerosol particles and fog - diversity of oceanic sources and atmospheric transformations, Atmos. Chem. Phys., 23, 15561–15587, https://doi.org/10.5194/acp-23-15561-2023, 2023.

Zeppenfeld, S., Schaefer, J., Pilz, C., Ebell, K., Zeising, M., Stratmann, F., Siebert, H., Wehner, B., Wietz, M., Bracher, A., and van Pinxteren, M.: Marine carbohydrates and other sea spray aerosol constituents across altitudes in the lower troposphere of Ny-Ålesund, Svalbard, Atmos. Chem. Phys., 26, 7235–7260, https://doi.org/10.5194/acp-26-7235-2026, 2026.

Zhao, S., Yan, J., Lin, Q., Yao, L., Park, K., Jung, J., Chen, L., Xu, S., Sun, M., Wang, S., Yang, H., Shi, J., Zhang, M., and Sun, H.: Changes in aerosol particle composition during sea fog formation events in the sea ice regions of the Arctic Ocean, Atmos. Environ., 272, https://doi.org/10.1016/j.atmosenv.2022.118943, 2022.

Zieger, P., Heslin-Rees, D., Karlsson, L., Koike, M., Modini, R., and Krejci, R.: Black carbon scavenging by low-level Arctic clouds, Nat. Commun., 14, https://doi.org/10.1038/s41467-023-41221-w, 2023.

Ziemba, L. D., Griffin, R. J., Whitlow, S., and Talbot, R. W.: Characterization of water-soluble organic aerosol in coastal New England: Implications of variations in size distribution, Atmos. Environ., 45, 7319–7329, https://doi.org/10.1016/j.atmosenv.2011.08.022, 2011.